Scientific Reports

https://doi.org/10.1038/s41598-026-66623-w

Article in Press

Application of artificial neural networks for prediction modeling and analysis of the thermophysical properties of Fe_3O_4/water ferrofluid using experimental measurement

Received: 27 March 2026

Accepted: 10 August 2026

Published online: 23 August 2026

Cite this article as: Abbas A.D., Basem A., Khalaf M.I. *et al.* Application of artificial neural networks for prediction modeling and analysis of the thermophysical properties of Fe_3O_4/water ferrofluid using experimental measurement. *Sci Rep* (2026). https://doi.org/10.1038/s41598-026-66623-w

Areej. D. Abbas, Ali Basem, Mohammed I. Khalaf, Narinderjit Singh Sawaran Singh, Farah Qasim Ahmed Alyousuf, Laith S. Sabri, Dheyaa J. Jasim, Mohamad Khaje khabaz, Mahmut Taner & Mohammad Tavalei

We are providing an unedited version of this manuscript to give early access to its findings. Before final publication, the manuscript will undergo further editing. Please note there may be errors present which affect the content, and all legal disclaimers apply.

If this paper is publishing under a Transparent Peer Review model then Peer Review reports will publish with the final article.

ARTICLE IN PRESS

© The Author(s) 2026. **Open Access** This article is licensed under a Creative Commons Attribution 4.0 International License, which permits use, sharing, adaptation, distribution and reproduction in any medium or format, as long as you give appropriate credit to the original author(s) and the source, provide a link to the Creative Commons licence, and indicate if changes were made. The images or other third party material in this article are included in the article's Creative Commons licence, unless indicated otherwise in a credit line to the material. If material is not included in the article's Creative Commons licence and your intended use is not permitted by statutory regulation or exceeds the permitted use, you will need to obtain permission directly from the copyright holder. To view a copy of this licence, visit http://creativecommons.org/licenses/by/4.0/.

ARTICLE IN PRESS

Application of Artificial Neural Networks for Prediction Modeling and Analysis of the Thermophysical Properties of Fe_3O_4/Water Ferrofluid Using Experimental Measurement

1. Areej. D. Abbas
College of Chemical Engineering, University of Technology- Iraq, Baghdad 10066, Iraq

Areej.d.abbas@uotechnology.edu.iq
2. Ali Basem
Advanced Technical College, University of Warith Al-Anbiyaa, Karbala, Iraq
Ali.basem@uowa.edu.iq

3. Mohammed I. Khalaf
Department of Computer Sciences, College of Science, University of Al Maarif, Al Anbar,31001, Iraq
m.i.khalaf@uoa.edu.iq

4. Narinderjit Singh Sawaran Singh
Faculty of Data Science and Information Technology, INTI International University, Persiaran Perdana BBN, Putra Nilai, Nilai 71800, Malaysia.
narinderjits.sawaran@newinti.edu
5. Farah Qasim Ahmed Alyousuf
Department of Computer Engineering, College of Engineering and Computer Science, Lebanese French University, Erbil, Kurdistan Region, Iraq.
frhalyousuf@lfu.edu.krd
6. Laith S. Sabri
College of Chemical Engineering, University of Technology- Iraq, Baghdad 10066, Iraq
laith.s.sabri@uotechnology.edu.iq
7. Dheyaa J. Jasim
College of Engineering, University of Al Maarif, Al Anbar,31001, Iraq.
dheyaa.jumaah@uoa.edu.iq
8- Mohamad Khaje khabaz
Department of Mechanical Engineering, Khomeinishahr Branch, Islamic Azad University, Khomeinishahr, Iran

9- Mahmut Taner
Istanbul Gelisim University, Department of Web Design and Development, 34310, Istanbul, Turkiye.
mtaner@gelisim.edu.tr

10- Mohammad Tavalei*

Fast Computing Center, Shabihsazan Ati Pars, Tehran, Iran
Mohammad.Tavalei@outlook.com
***Corresponding Author: Mohammad Tavalei;** Mohammad.Tavalei@outlook.com

Abstract

The use of nanofluids has attracted significant attention due to their improved thermal performance compared with conventional heat transfer fluids. Because nanoparticles are on the nanometer scale, problems such as channel blockage and severe abrasion can be reduced. Among these, Ferrofluid containing Fe_3O_4 nanoparticles is of particular interest to researchers due to its unique properties, including favorable magnetic properties and environmental friendliness. In this study, an artificial neural network model is

ARTICLE IN PRESS

developed to predict the thermal behavior of Fe_3O_4/Water Ferro-nanofluid, and the effective factors, such as volume fraction (φ = 0.05% to 4.0%) and temperature (T = 24 °C to 50 °C), on thermal conductivity and dynamic viscosity are investigated. The performance of the ANN is validated by comparing the obtained results. The results show that when the φ changes from φ = 0.05% to 4.0%, the dynamic viscosity increases from 0 cP to 0.77 cP. The results showed that thermal conductivity increased with increasing nanoparticle concentration, while dynamic viscosity decreased with increasing temperature. In contrast, viscosity increased at higher nanoparticle volume fractions due to stronger particle interactions within the base fluid. The ANN models showed reasonable overall performance in estimating thermal conductivity, with correlation coefficients of 0.98 and errors of 1.56×10^{-5}.

Keywords: Artificial Neural Network (ANN); Fe_3O_4/Water Ferrofluid; Dynamic Viscosity; Thermal Conductivity.

Table of nomenclatures

Symbol	Description	Unit
T	Temperature	°C
φ	Nanoparticle volume fraction	%
k	Thermal conductivity	W/m·K
μ	Dynamic viscosity	cP
ANN	Artificial Neural Network	–
MLP	Multi-Layer Perceptron	–
x_i	Input variable of the ANN model	–
y_k	Output variable of the ANN model	–
w_{ijk}	Weight coefficient between neurons	–
b_{ik}	Bias term of the neuron	–
$f(x)$	Activation function	–
i, j, k	Indices representing neurons in different layers	–
MSE	Mean Squared Error	–
R	Correlation coefficient	–

ARTICLE IN PRESS

1. Introduction

Fluids like water and oil have limited heat transfer capacity. However, metals have thermal conductivities up to three times higher than those of these fluids . Combining these two materials yields a fluid with the thermal conductivity of metals [1]. With the advent of nanofluids, researchers and experts in heat transfer hope that energy conversion will be faster and more efficient using these materials [2, 3]. Nanofluids are suspensions obtained by mixing solid nanoparticles with liquids to improve or create new properties. Because the particle size of

ARTICLE IN PRESS

nanofluids is on the scale of fluid molecules [4], using smaller nanofluid particles in the nanometer range can better prevent abrasion and channel blockage [5, 6]. With the advancement of nanofluid research, nanofluids can also be produced by adding metal oxide nanoparticles and CNTs [7]. The addition of nanoparticles to the fluid affects thermophysical properties, including heat capacity, heat transfer coefficient, thermal conductivity, nanofluid stability, viscosity, pH, and density [8]. In addition, increasing the concentration of nanoparticles reduces nanofluid stability, leading to particle deposition on mechanical surfaces and damage to the mechanical system .

Among these, nanofluids containing Fe_3O_4 nanoparticles are of particular interest to researchers due to their unique properties, including favorable magnetic properties and environmental friendliness [9]. Sundar et al. [10] studied the thermophysical properties of Fe_3O_4/water magnetic nanofluids. The results show that the nanofluid's thermal properties and viscosity improved. Shahsavar and Behiraei[11] investigated the thermal conductivity and viscosity of water-based composite nanofluids containing Fe_3O_4 and CNT. Process influencing factors included temperature (25-55 °C), the volume fraction of Fe_3O_4 nanoparticles (φ =0.1 to 0.9%), and the volume fraction of CNT nanoparticles (φ = 0 to 1.35%). The increase in viscosity is inversely related to the shear rate and to the addition of nanoparticles. In recent years, ANN, RSM, GA, and other modeling methods have been used extensively in heating systems. Artificial neural networks in heating systems have recently been applied to laboratory data and thermophysical properties of nanofluids and have been able to estimate laboratory data with high accuracy or estimate the efficiency or control of heating systems' dynamics [2, 12, 13]. ANNs are powerful, flexible functions and a powerful method for analyzing data and modeling nonlinear relationships with high accuracy [14, 15]. ANNs have a unique ability to learn and discover relationships, which are used in all engineering sciences as powerful tools for simulating phenomena. In this method,

ARTICLE IN PRESS

observation data are incorporated into the model, and after training, the forecasts and simulations achieve appropriate accuracy. In most cases, the results are successful and acceptable [16-19]. Esfe et al. [13] investigated the thermal conductivity of hybrid nanofluids. They used the laboratory results to train an ANN, and the experimental relationships to estimate thermal conductivity values. They employed two types of multilayer perceptron ANNs and radial basis function approximation. Tian et al. [12] used an ANN to investigate the thermal properties of a hybrid nanofluid. They extracted nanofluid thermal-conductivity results from six nanoparticle volume fractions and seven temperatures. In addition, they used 10 different algorithms to train ANNs. They reported an average MSE of 1.67×10^{-6} and a correlation coefficient of 0.999 using the ANN. Their result indicated that the effect of temperature on changing thermal conductivity is more significant than φ. The results show that increasing the φ and temperature has a positive effect on thermal properties. Rostami et al. [20] simulated the thermal properties of MWCNT-CuO/water nanofluid using ANNs, and the results show that by increasing the temperature to T=50 °C and φ=0.6%, the heat transfer improves. Kumar et al. [21] investigated the heat transfer of alpha-alumina/water nanofluid. The results show that the addition of Al_2O_3 nanoparticles significantly increases the heat transfer coefficient. Nanofluid viscosity is a significant parameter in fluid transfer. Determination of nanofluid viscosity is necessary to accurately calculate the pumping power and Reynolds number [22]. According to studies, adding nanoparticles increases viscosity. For example, Qing et al. [2] examined the dynamic viscosity of Al_2O_3-MWCNT (40:60)/Oil SAE50 nanofluid at various temperatures and φ using ANN. The results show that the φ had a negligible effect on the dynamic viscosity, especially at higher temperatures. The MSE values and correlation coefficients were 3.58 and 0.999, respectively. Goodarzi et al. [23] investigated the viscosity of the hybrid nanofluid in the ZnO-MWCNT/SAE 10W40 engine. The results show that the

ARTICLE IN PRESS

nanofluid's viscosity was directly related to the increase in φ and inversely related to the increase in temperature. Esfe et al. [24] predicted the dynamic viscosity of MWCNT–Al_2O_3 (30–70%)/oil SAE40 hybrid nanofluid using ANN. The correlation coefficient and MSE were 0.99.

Fe_3O_4/water ferrofluid has attracted considerable attention in recent years because it combines the magnetic properties of Fe_3O_4 nanoparticles with the favorable heat-transfer characteristics of water. Due to these features, this type of Ferrofluid has been widely considered for applications such as compact cooling systems, heat exchangers, electronic thermal management, and biomedical processes, including magnetic hyperthermia. Previous studies have shown that the thermophysical properties of Fe_3O_4/water ferrofluids, particularly thermal conductivity and dynamic viscosity, are strongly influenced by both temperature and nanoparticle concentration. In addition, factors such as particle agglomeration, Brownian motion, surfactant type, and suspension stability can significantly affect the experimental results. Therefore, conventional empirical correlations and classical theoretical models are often limited to specific operating conditions and may not accurately capture the nonlinear behavior of ferrofluids across broader ranges of temperature and concentration. Although several machine-learning and ANN-based approaches have recently been proposed for predicting the properties of Fe_3O_4/water nanofluids, many of these studies focused on a single thermophysical property or used limited datasets and narrow operating ranges [25]. In the present study, an ANN-based prediction model is developed to simultaneously predict the thermal conductivity and dynamic viscosity of Fe_3O_4/water ferrofluid using temperature and nanoparticle volume fraction as the main input parameters. The proposed model provides a reliable and flexible approach for capturing the Ferrofluid's nonlinear thermophysical behavior over the studied operating conditions.

ARTICLE IN PRESS

Based on previous studies on improving heat transfer behavior in nanofluids using methods such as computer simulations and the ANN method, it can be said that far too little attention has been paid to the properties of Fe_3O_4/Water Ferrofluid. In addition, the selected concentration and temperature ranges allow the model to capture both dilute and highly concentrated ferrofluid behavior, making the proposed approach more comprehensive and practically applicable for thermal engineering systems.

In this study, an ANN model is developed to predict the thermal behavior of Fe_3O_4/Water Ferrofluid, and the effective factors, including φ and temperature-dependent thermophysical properties, are investigated. Also, using ANNs, relationships are provided to estimate and predict the thermal conductivity and dynamic viscosity of Fe_3O_4/Water Ferrofluid.

2. Methodology

2.1. Preparation of Fe_3O_4/water ferrofluid

So far, various methods have been studied for preparing nanoparticles or dispersing them in a fluid. However, two single-step and two-step methods are often used to make nanofluids. One common method for preparing nanofluids is the two-step method. This is a physical method that involves adding nanopowder to the fluid. Since then, industries have produced enough nanopowders on a commercial scale, making this method widespread [26]. There are several methods for producing nanoparticles, the most widely used being gas-phase condensation. In this method, nanoparticles or nanotubes are usually prepared by chemical vapor deposition (CVD) in an inert gas atmosphere, forming dry powders. Then the nanoparticle or nanotube is dispersed into the fluid. For this purpose, methods such as ultrasonic vibration or surfactant addition are used to reduce nanoparticle mass and improve dispersion behavior. The two-step method is very suitable for some cases, such as metal oxide in deionized water, but has been less successful for nanofluids containing heavy-

ARTICLE IN PRESS

metal nanoparticles [27]. One advantage of nanofluid production via the two-step inert gas condensation method, which involves evaporating materials under vacuum, is that it minimizes nanoparticle accumulation. The two-step method has potential economic benefits, because many companies can produce nanopowders on an industrial scale. In this research, a two-step method has been used to produce nanofluids. First, iron oxide nanoparticle powder was prepared and mixed with deionized water-based fluid (DW) to form a nanofluid. In this work, laboratory results were used to predict the thermal conductivity and dynamic viscosity of a Fe_3O_4/water nanofluid using an ANN. The mass of nanoparticles required for each prescribed volume fraction was calculated using the densities of the nanoparticles and base fluid. The nanoparticles were weighed using an analytical balance and gradually added to the measured quantity of deionized water. Each suspension was initially mixed. Subsequently, the mixture was sonicated using a probe ultrasonicator operating. During sonication, the sample temperature was maintained to prevent evaporation and temperature-induced changes in the suspension [28].

A Brookfield DV2 viscometer was used to measure the dynamic viscosity of the prepared nanofluid samples. The instrument determines and directly displays viscosity under specified rotational conditions and can operate at rotational speeds of up to 1000 rpm. The measured viscosity is reported in centipoise (cP), which is equivalent to mPa·s. The instrument provides a stated measurement accuracy of ±0.1%. The Brookfield DV2 viscometer and the experimental measurement arrangement are presented in Fig 1.

ARTICLE IN PRESS



Fig.1. Brookfield model DV2 Viscometer

The temperature range of 24–50 °C was selected because it represents the typical working conditions of many water-based ferrofluid heat transfer systems. Temperatures near room temperature and slightly higher are commonly used in practical cooling and thermal applications. In addition, using temperatures outside this range could lead to suspension instability and increase the effect of natural convection during measurements, potentially reducing the accuracy of the experimental data. The nanoparticle concentration range of 0.05–4% was chosen to study the behavior of the Ferrofluid from very low particle loading up to relatively high concentrations. At low concentrations, the fluid properties remain close to those of pure water, whereas at higher concentrations, particle interactions become more significant, affecting thermal conductivity and viscosity. Selecting this range enabled evaluation of both the improvement in thermal performance and the corresponding changes in flow behavior across different operating conditions.

2.2. ANN structure

A three-layer feed-forward ANN, consisting of the input layer (IL), the hidden layer (HL), and the output layer (OL), predicts two variables of OL. Initially, input data (temperature and φ) were introduced to the IL. Therefore, the IL has two neurons. These neurons are joined to HL by

ARTICLE IN PRESS

connection weights (CW), which signal HL neurons. The strength of each signal is dependent upon the CWs and other elements like bias and the activation function (AF) of each neuron. Then the CWs sum in HL neurons, and the bias is added. A bias value is provided to add a constant to the weighted input values [29]. These values are forwarded within the ANN model along the HL neurons, which finally generate the output data after passing through the AF. The bias is used to adjust the output and the weighted sum of the inputs to the neurons, allowing the activation function to be shifted left or right to better fit the target data. Therefore, the weights are changed in proportion to the negative of an error derived from each weight [15, 30]. The HL at that point relates to the OL that produces the output from the AF. It can be noted that AFs include nonlinear and linear equations, and AF between the HL and OL is expressed as [31]:

$$F_k = f\sum_{j=1}^{q}\left(w_{ijk}x_j + b_{ik}\right) \qquad k=1,2,\ldots.m \tag{1}$$

$$Y_i = \left(\sum_{k=1}^{m} w_{ok}F_K\right) + b_0 \tag{2}$$

Where x_j represents the input parameter of the network, and w_{ijk} , b_{ik} , q, and f denote the weighting coefficient connecting neurons between successive layers, bias matrices, number of input variables, and transfer function, respectively. In addition, n indicates the number of neurons in the hidden layer, while $f(x)$ denotes the activation (transfer) function applied during the learning process. The symbols i, j, and k are indices corresponding to the input layer, hidden layer, and output layer neurons, respectively. The OL determines the weighted sum of the signals from the HL, and the associated coefficients are grouped into the matrices W_{ok} and b_0. The dataset was obtained from 100 experimental measurements. In this simulation, 75% of the data is used to train the network, and the remaining 25% is split into a validation and a test set.

ARTICLE IN PRESS

The models in this work have been trained and evaluated on experimental measurements without explicitly propagating input measurement errors. In practice, experimental uncertainties in temperature and nanoparticle concentration will induce corresponding uncertainties in the predicted thermal conductivity and viscosity. To quantify this, one can use sampling or ensemble methods, for example, by drawing many random perturbations of each input (within its measurement error) and propagating them through the fixed ANN; a distribution of outputs is obtained, from which 95% prediction intervals can be computed. Similarly, training multiple ANNs on bootstrapped datasets or employing Monte Carlo dropout yields a spread of predictions reflecting model uncertainty. In the current study (100 data points, 75/25 split), we did not explicitly perform this analysis, but the very low errors (high R^2) suggest that input noise would produce very narrow output distributions. As a concrete next step, we recommend that future studies run a Monte Carlo propagation: e.g., assume ±1% input noise, sample 10,000 perturbed inputs per test point, and compute the mean and 95% CI of the ANN outputs. A similar approach is to train an ensemble of ~20–50 networks (via bootstrapping or different initial seeds) and report mean±std of predictions. These intervals can be visualized (e.g., in calibration plots) to verify that ~95% of observed properties fall within the predicted 95% intervals. Such analyses would concretely demonstrate the impact of experimental uncertainty on model predictions and enhance the reported results without changing the underlying model architectures.

The 20 networks were obtained by trial and error after testing different numbers of hidden-layer nodes. Table 1 tabulates the experimental dataset of Fe_3O_4/Water Ferrofluid.

Table 1. The experimental dataset of Fe_3O_4/Water Ferrofluid.

	Thermal Conductivity									
Temperature	0.250-0.253	0.253-0.256	0.256-0.259	0.259-0.262	0.262-0.265	0.265-0.268	0.268-0.271	0.271-0.274	0.274-0.277	0.277-0.280

ARTICLE IN PRESS

					Volume fraction 0.1%					
25-30	0.704	0.645								
30-35			0.577							
35-40					0.523					
40-45								0.470		
45-50										0.433
	Thermal Conductivity									
	0.250-0.253	0.253-0.256	0.256-0.259	0.259-0.262	0.262-0.265	0.265-0.268	0.268-0.271	0.271-0.274	0.274-0.277	0.277-0.280
Temperature					Volume fraction 0.2%					
25-30	0.724	0.662								
30-35				0.595						
35-40					0.540					
40-45						0.478				
45-50							0.475	0.440	0.455	
	Thermal Conductivity									
	0.250-0.253	0.253-0.256	0.256-0.259	0.259-0.262	0.262-0.265	0.265-0.268	0.268-0.271	0.271-0.274	0.274-0.277	0.277-0.280
Temperature					Volume fraction 0.3%					
25-30		0.745	0.679							
30-35				0.610	0.562					
35-40						0.560				
40-45						0.495	0.503			
45-50									0.467	
	Thermal Conductivity									
	0.250-0.253	0.253-0.256	0.256-0.259	0.259-0.262	0.262-0.265	0.265-0.268	0.268-0.271	0.271-0.274	0.274-0.277	0.277-0.280
Temperature					Volume fraction 0.4%					
25-30		0.763	0.686				0.632			
30-35										
35-40					0.625					
40-45							0.560	0.554		
45-50								0.516		0.482

ARTICLE IN PRESS

The Fe_3O_4 volume fraction was deliberately limited to 0.05–4.0% in the experiments and ANN modeling. This range covers the dilute regime where the Ferrofluid remains stable and Newtonian under our preparation conditions. We chose 0.05% as a practical lower bound (below this, conductivity changes are within noise) and 4.0% as an upper bound to avoid excessive viscosity increases and particle aggregation. Prior studies similarly focus on concentrations of just a few percent by volume. Above this regime, nanofluid behavior changes qualitatively (strong non-Newtonian effects, clustering, and sedimentation may occur), and additional input descriptors

ARTICLE IN PRESS

(e.g., surfactant content or shear rate) would be needed. Thus, the selected range ensures that our model remains in a domain of nearly continuous, well-dispersed fluid, consistent with the single-experiment dataset and the literature on magnetic nanofluid.

The network architectures (MLP 2-3-2 and 2-4-2) were selected after systematic evaluation of several candidate MLPs. We tested single-hidden-layer networks with 2–5 neurons, using both logistic sigmoid and hyperbolic tangent functions in the hidden layer and an exponential function in the output layer to ensure positive outputs3. Training employed the BFGS quasi-Newton algorithm (MATLAB's trainbfg), which updates weights by approximating the Hessian and converges rapidly for small to medium networks. A random 75%/25% split of the data was used for training/validation/test (with a fixed random seed for reproducibility). The validation set monitored performance, and training was stopped if the validation error did not improve for 6 consecutive checks. We selected the final MLP 2-3-2 and 2-4-2 architectures because they minimized the validation mean-squared error and maximized R^2 while avoiding overfitting, consistent with the rule-of-thumb that hidden neurons be between the input and output sizes (and typically not exceed twice the input size).

ARTICLE IN PRESS

The output can be compared with the experimental values, and the error (difference between the target and the output) is subsequently calculated. The error data is continuously sent backward from the OL to the IL via the HLs. A training algorithm learns a decision function that updates the ANN's weights. Hence, the training requires updating the weights and biases of each neuron in the backpropagation network to reduce signal latency. An epoch occurs when the training vectors are used to update the ANN's weights in a single step. This iterative approach updates the network's weights across the various vectors at different times until the error between the computed and experimental values reaches a minimum and the required accuracy is achieved. In the current work,

ARTICLE IN PRESS

the BFGS algorithm was employed. BFGS is a second-order optimization algorithm. It is an abbreviation of the four algorithm encoders: Broyden, Fletcher, Goldfarb, and Shanno. BFGS is the most popular gradient descent algorithm that determines the downward direction by pre-processing the gradient with curvature information.

3. Results

To investigate the effect of temperature and φ, T=25 to 50 ˚C and φ=0.05-4% were selected. The influence of temperature and φ on the thermal conductivity and dynamic viscosity of Fe3O4/Water Ferrofluid was investigated in Fig. 2. In Fig. 2a, the thermal conductivity ranges for each φ were determined and compared. Unlike thermal conductivity, viscosity has its lowest value at high temperatures. However, as φ increases, the lack of thermal conductivity is slightly compensated. The viscosity increase is the same at all temperatures. The dynamic viscosity values for each fraction are determined and compared. As shown in Fig. 2b, at low temperatures, the thermal conductivity is at its lowest level. The 3D contour plots provide a graphical representation of the combined effects of two independent variables on the response parameter while keeping the third parameter constant. These plots clearly illustrate the interaction between variables and help identify the regions associated with maximum and minimum response values. The smooth surface distribution and contour gradients indicate good consistency between the experimental observations and the developed predictive model. However, because the φ will increase, Fe_3O_4/Water Ferrofluid turns into a more thermally efficient. The increase in thermal conductivity at any temperature follows a similar pattern. It has also been determined that with a small φ, the slope of the increase in thermal conductivity is greater with increasing temperature. At excessive temperatures, the maximum value of thermal conductivity is reached as φ increases to the

ARTICLE IN PRESS

maximum value. In addition, Figs. 2c and 2d show the effect of φ on the dynamic viscosity of Fe_3O_4/Water ferrofluid at various temperature ratios, where φ ranges from 0.05% to 4.0%; the dynamic viscosity increases from 0.43 to 0.77 cP.

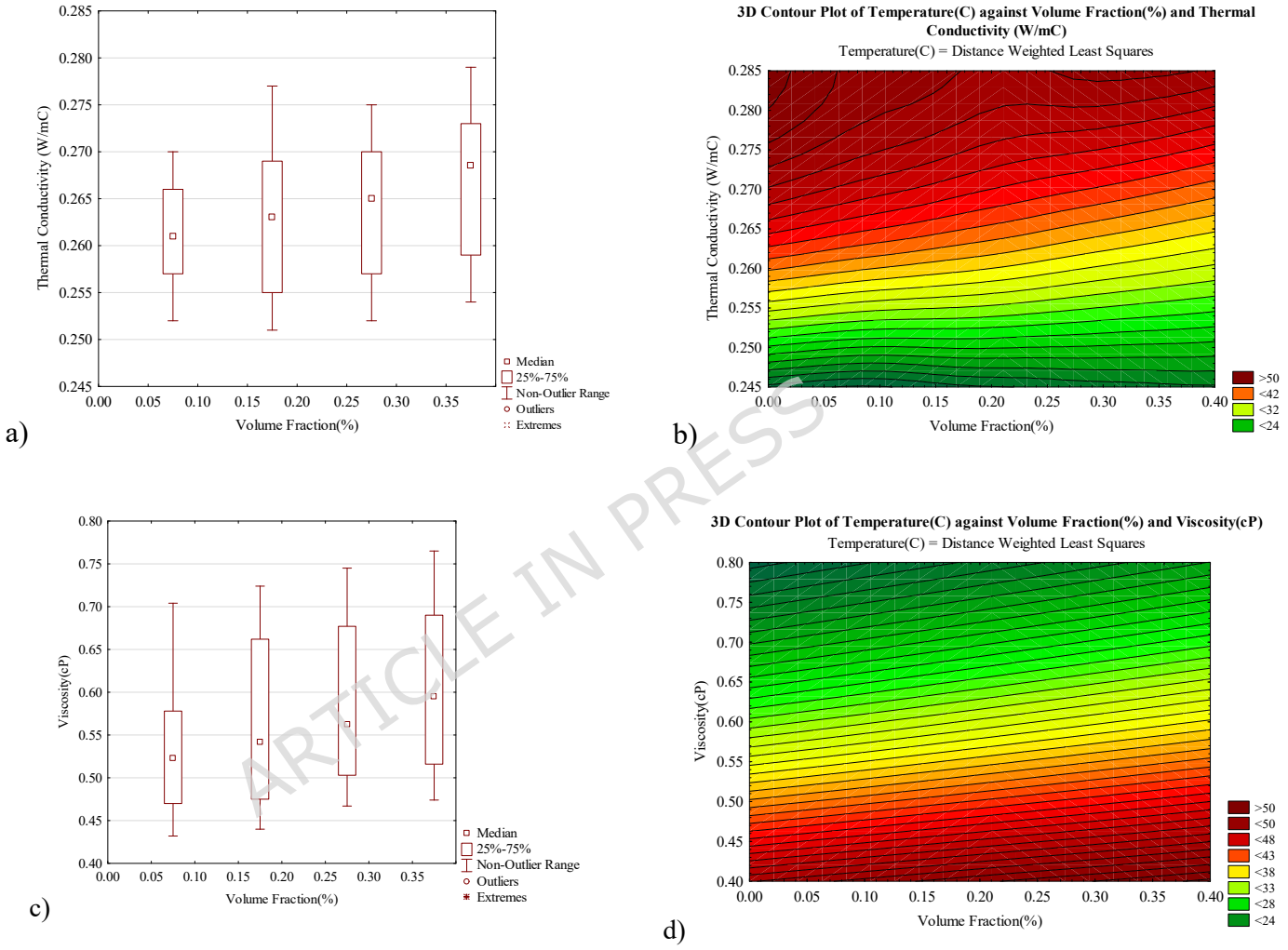


Fig. 2. Volume fraction changes in thermal conductivity and dynamic viscosity.

Fig. 3 shows the effect of temperature changes on the thermal conductivity and dynamic viscosity of Fe_3O_4/Water Ferrofluid and the 3D contour plot of φ as a function of temperature and thermal conductivity. Fig. 3b indicates that excessive thermal conductivity can be achieved at low temperatures if the highest φ. The figure shows that by exceeding the temperature of 30 °C, high thermal conductivity can be achieved even in small proportions of the φ. Fig. 3d shows that with

ARTICLE IN PRESS

increasing temperature, the dynamic viscosity in all φ groups decreases with the same gradient. The upward trend in thermal conductivity and the downward trend in viscosity, along with their variations at each temperature, are shown in Figs. 3a and 3c. The results show that thermal conductivity increases gradually with increasing nanoparticle concentration because Fe_3O_4 nanoparticles possess higher thermal conductivity than the base fluid. In addition, increasing the temperature enhances nanoparticles' Brownian motion, thereby improving heat transport within the suspension. The smooth trend observed in the figure indicates stable thermal behavior. Moreover, viscosity increases with increasing nanoparticle loading due to stronger interaction and friction between suspended particles. On the other hand, increasing temperature reduces viscosity because higher thermal energy weakens intermolecular forces, thereby increasing fluid mobility. The figure clearly demonstrates the combined influence of temperature and concentration on the rheological behavior of the Ferrofluid [32].

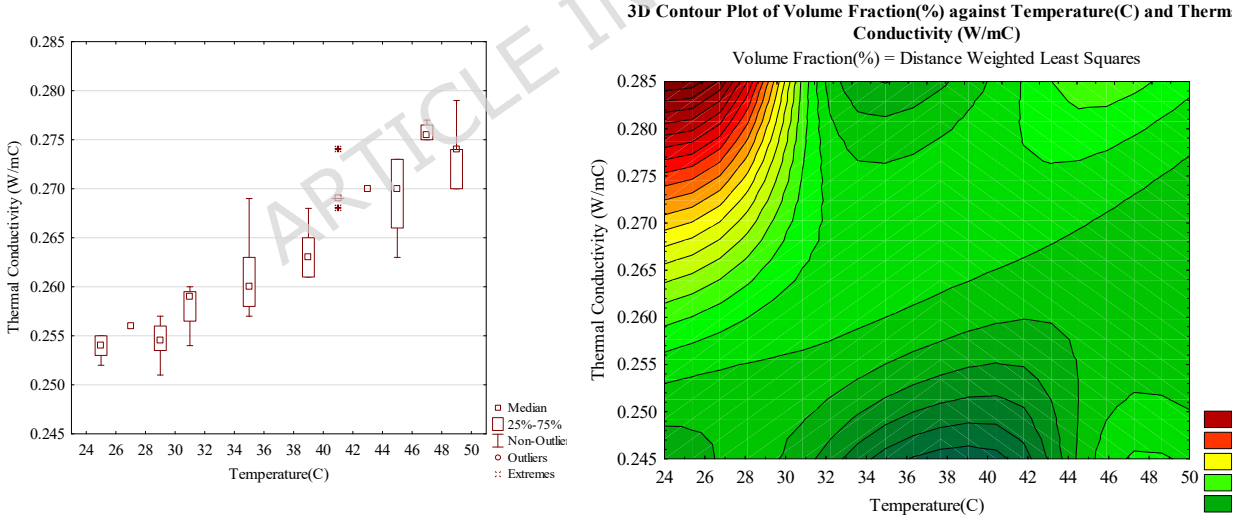
The observed viscosity behavior of the Fe_3O_4/water ferrofluid is consistent with classical suspension rheology. The dynamic viscosity increased with nanoparticle volume fraction and decreased with increasing temperature. The reduction in viscosity at elevated temperatures can be attributed to a decrease in the base-fluid viscosity due to weakened intermolecular forces and enhanced molecular mobility. Conversely, increasing the nanoparticle concentration increased hydrodynamic resistance and particle-fluid interactions, leading to higher viscosity. For dilute suspensions, the experimental results are in good agreement with Einstein's classical model, which predicts a linear increase in viscosity with particle volume fraction. At higher concentrations, slight deviations from linearity become apparent due to increased particle interactions, and the observed trend is more accurately described by semi-empirical models such as the Batchelor and Krieger–Dougherty correlations. These models account for hydrodynamic interactions and crowding

ARTICLE IN PRESS

effects that become significant as the nanoparticle loading increases. The measured viscosity values, therefore, fall within the range predicted by established viscosity theories for dispersed particle suspensions.

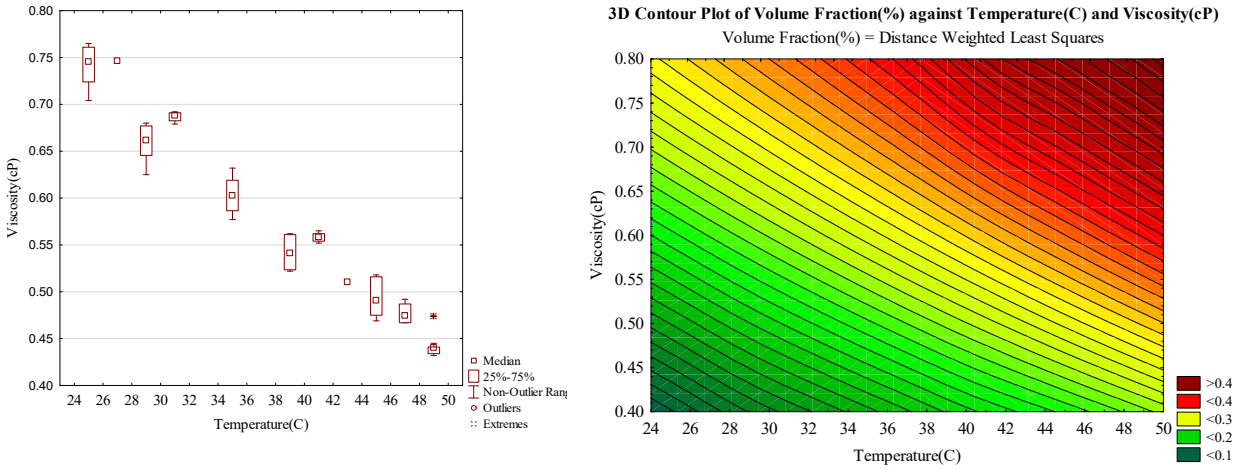
Furthermore, no evidence of abnormal rheological behavior, such as shear-thinning, shear-thickening, or field-induced particle chaining, was observed within the investigated temperature range (24–50 °C) and volume fraction range (0.05–4.0%). This suggests that the Fe_3O_4 nanoparticles remained sufficiently dispersed in the base fluid and that the Ferrofluid behaved predominantly as a Newtonian suspension. Overall, the agreement between the experimental observations and the classical Einstein, Batchelor, and Krieger–Dougherty models confirms that viscosity trends are primarily governed by particle concentration effects and the temperature-dependent viscosity of the water-based fluid [26].

ARTICLE IN PRESS



(a) (b)

ARTICLE IN PRESS



(c) (d)

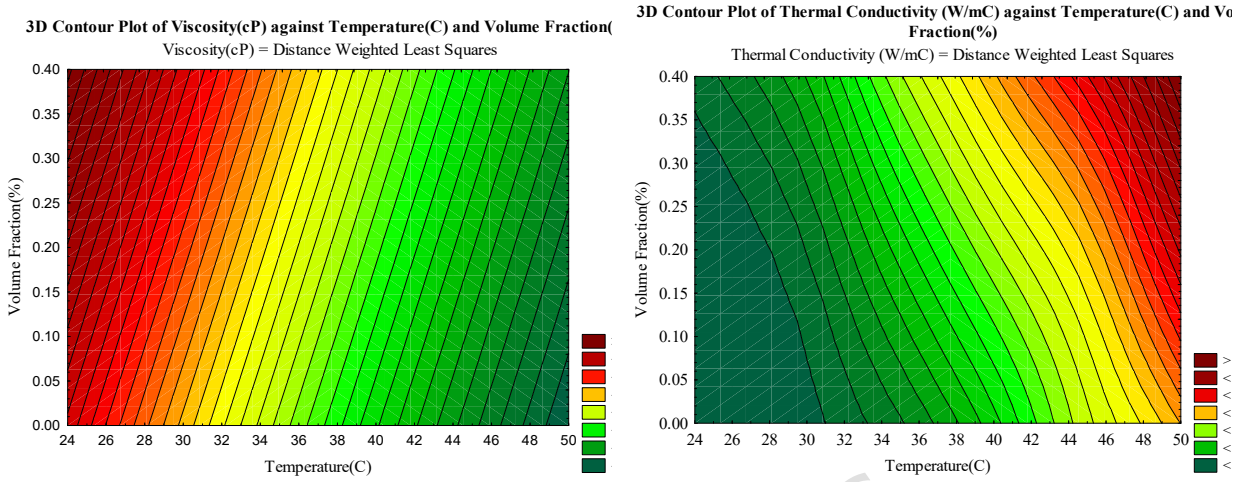
Fig. 3. Temperature variation on the Fe_3O_4/Water Ferrofluid thermal conductivity and dynamic viscosity

The effect of temperature and φ on thermal conductivity and dynamic viscosity of Fe_3O_4/Water Ferrofluid to determine their maximum and minimum values can be seen in Fig. 4.

The enhanced thermal conductivity of Fe_3O_4/water nanofluids is attributed to several effects. The studies identify Brownian-motion-induced nanoconvection, interfacial liquid layering, and particle clustering/percolation as key mechanisms. In the low-concentration regime of our study, we expect static conduction enhancements to dominate. Specifically, the thermal conductivity increases roughly linearly with φ, implying that each additional nanoparticle adds conductive paths to the network. If particles aggregate or form loose chains, they can create short-circuits for heat flow8. Interfacial liquid layers around each nanoparticle may also conduct better than bulk water due to structured ordering. By contrast, purely Brownian effects are predicted to be minor: the ratio of thermal diffusion to Brownian motion is large, so random motion does not contribute significantly. In practice, measured enhancements for Fe_3O_4/water at $\varphi \leq 5\%$ are modest (tens of percent) and scale with concentration, consistent with conduction along particle networks. We therefore

ARTICLE IN PRESS

interpret our results as arising mainly from improved connectivity (and possibly a nanolayered interface) rather than micro-scale convection.



(a) (b)

Fig. 4. Effect of temperature changes on the Fe_3O_4/Water Ferrofluid thermal conductivity

To assess the training value of the ANN, a range of hidden-layer neuron counts and a unique set of networks were designed, as shown in Table 2. The error rates and training performance of 20 ANN models were calculated using MATLAB. The Minimum Mean Squared Error (MSE) performance was found for these ANNs. In this table, 20 MLP–ANN pairs were trained. The evaluation of the error values for each ANN is a good indicator of training performance, as shown in Table 2.

Table 2. Comparison of the prepared values of simulated ANNs' error and correlation.

No.	ANNs	Training perf.	Test perf.	Validation perf.	Train error	Test error	Validation error
1	MLP 2-7-2	0.991584	0.974815	0.979314	6.77×10^{-6}	6.10×10^{-6}	4.98×10^{-6}
2	MLP 2-4-2	0.963109	0.960045	0.965091	2.96×10^{-4}	2.10×10^{-4}	1.18×10^{-4}
3	MLP 2-9-2	0.992151	0.975773	0.979009	4.20×10^{-6}	5.03×10^{-6}	5.05×10^{-6}
4	MLP 2-4-2	0.990473	0.976804	0.978377	2.41×10^{-5}	1.51×10^{-5}	1.56×10^{-5}
5	MLP 2-4-2	0.976786	0.965621	0.966811	2.07×10^{-4}	1.00×10^{-4}	1.73×10^{-4}
6	MLP 2-3-2	0.967294	0.970204	0.957546	3.23×10^{-4}	1.51×10^{-4}	3.00×10^{-4}
7	MLP 2-7-2	0.985367	0.973337	0.975362	4.97×10^{-5}	5.98×10^{-5}	5.12×10^{-5}
8	MLP 2-5-2	0.983210	0.976801	0.973686	2.98×10^{-5}	2.28×10^{-5}	1.53×10^{-5}

ARTICLE IN PRESS

9	MLP 2-4-2	0.987987	0.974309	0.981240	5.62×10^{-6}	5.84×10^{-6}	4.35×10^{-6}
10	MLP 2-6-2	0.989175	0.973162	0.970450	3.18×10^{-5}	1.73×10^{-5}	2.39×10^{-5}
11	MLP 2-8-2	0.976938	0.965795	0.966851	2.07×10^{-4}	1.00×10^{-4}	1.74×10^{-4}
12	MLP 2-9-2	0.992503	0.972843	0.979262	2.83×10^{-6}	7.03×10^{-6}	5.00×10^{-6}
13	MLP 2-3-2	0.992973	0.977399	0.978419	9.37×10^{-6}	5.28×10^{-6}	8.14×10^{-6}
14	MLP 2-3-2	0.990598	0.974590	0.976248	2.56×10^{-5}	1.32×10^{-5}	1.17×10^{-5}
15	MLP 2-5-2	0.962691	0.957814	0.964458	2.94×10^{-4}	2.14×10^{-4}	1.02×10^{-4}
16	MLP 2-9-2	0.990320	0.974653	0.977484	2.05×10^{-5}	2.07×10^{-5}	9.03×10^{-6}
17	MLP 2-7-2	0.992595	0.972687	0.976383	7.46×10^{-6}	3.75×10^{-5}	1.11×10^{-5}
18	MLP 2-3-2	0.961807	0.958264	0.964348	2.91×10^{-4}	1.96×10^{-4}	1.27×10^{-4}
19	MLP 2-6-2	0.992275	0.974845	0.976105	2.25×10^{-6}	4.32×10^{-6}	3.46×10^{-6}
20	MLP 2-5-2	0.990982	0.974559	0.979962	1.24×10^{-5}	8.21×10^{-6}	7.87×10^{-6}

The notation MLP (2-h-2) indicates a feed-forward multilayer perceptron containing two input neurons, (h) neurons in a single hidden layer, and two output neurons. Temperature and nanoparticle volume fraction constituted the two input variables, whereas thermal conductivity and dynamic viscosity were the two predicted outputs. Twenty candidate networks containing 3–9 hidden neurons were trained and evaluated under identical data-partitioning conditions. Model selection was not based exclusively on the minimum training error, since a very low training MSE does not necessarily indicate superior generalization. Instead, testing and validation performance, prediction error, and network complexity were considered simultaneously. Network 13, with an MLP 2–3–2 architecture, achieved the highest test-performance coefficient of 0.977399, while Network 4, with an MLP 2–4–2 architecture, produced the second-highest value of 0.976804. Although Network 19 generated lower MSE values, its six-neuron hidden layer did not improve the independent testing-performance coefficient. Consequently, the compact MLP 2–3–2 and MLP 2–4–2 architectures were selected because they provided the most suitable balance between predictive performance, generalization capability, and architectural parsimony.

The ANN with satisfactory performance is chosen as a result. Because ANNs' training weights are random, each ANN is trained on different instances using different methods, leading to a satisfactory system. Finally, the hidden layer has registered the most effective networks with three

ARTICLE IN PRESS

and four neurons (MLP 2-3-2 and MLP 2-4-2). To calculate the overall performance and error of the model, Eq. (3) is used.

$$MSE = \frac{1}{N}\sum_{i=1}^{N}(Y_{ANN} - Y_{ex})^2 \quad (3)$$

In which Y_{ANN} and Y_{ex} denote the predicted value of the ANN and the experimental value, respectively. Furthermore, in Eq. (3), N represents the number of sample data points. In the hidden layer, the activation function for MLP 2-3-2 and 2-4-2 is logistic. Similarly, the activation functions for the output layers are Tanh and exponential for MLPs 2-3-2 and 2-4-2, as shown in Eqs. (4) and (6) :

$$Tanh(x) = \frac{e^x - e^{-x}}{e^x - e^{-x}} \quad (4)$$

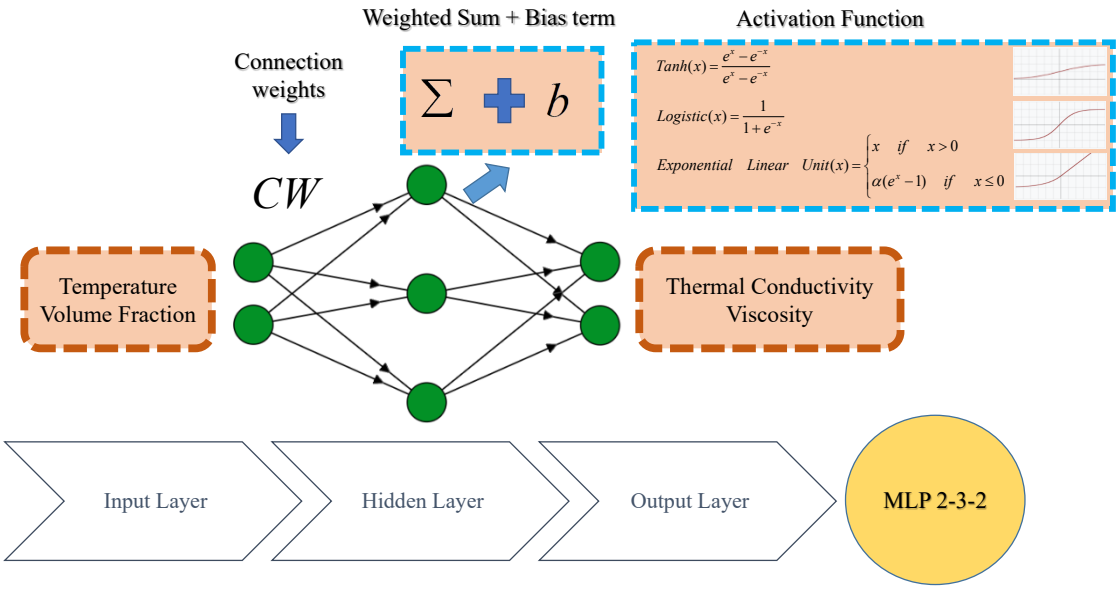
$$Logistic\ (x) = \frac{1}{1 + e^{-x}} \quad (5)$$

$$Expotential\ linear\ unit\ (x) = \begin{cases} x & if\ x > 0 \\ \alpha(e^x - 1) & if \quad x \leq 0 \end{cases} \quad (6)$$

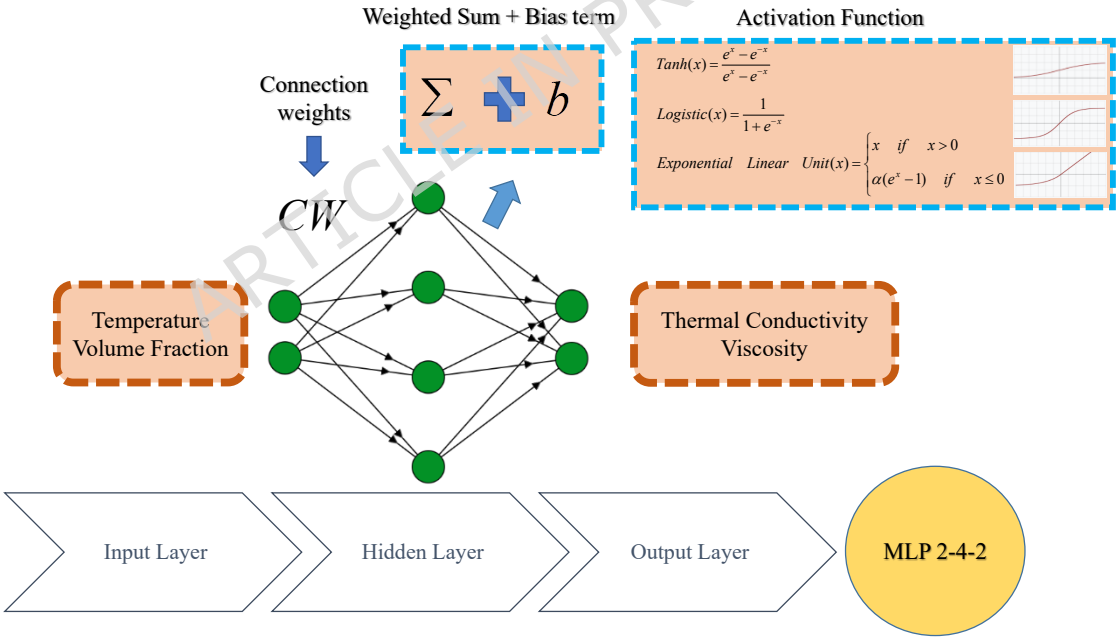
ARTICLE IN PRESS

Fig. 5 shows the schematic of an optimal ANN structure selected to predict the thermal conductivity and dynamic viscosity of a Fe_3O_4/Water Ferrofluid. ANNs 4 and 13 are the best training methods because they have the least error.

ARTICLE IN PRESS



(a)



(b)

Fig. 5. The schematic of a feed-forward ANN structure for predicting the thermal conductivity of Fe_3O_4/Water Ferrofluid (a) MLP 2-3-2 and (b) MLP 2-4-2

The selection of compact ANN architectures in this study was primarily motivated by the low dimensionality of the problem, where only two operating parameters, temperature and nanoparticle

ARTICLE IN PRESS

concentration, were used to predict two strongly correlated thermophysical properties. Previous nanofluid modeling studies have consistently identified these variables as the dominant factors affecting thermal conductivity and viscosity, particularly in Fe_3O_4/water systems. Under such conditions, a single hidden layer with a limited number of neurons is generally sufficient to capture the nonlinear input–output relationship. Another important consideration was the risk of overfitting relative to the dataset size. Earlier studies have reported that excessively large hidden layers may increase computational cost and reduce generalization performance, especially for datasets obtained from a single experimental campaign.

In contrast, compact architectures have shown satisfactory accuracy in several low-dimensional nanofluid studies. Furthermore, previous investigations demonstrated that performance improvements become marginal beyond approximately 4–5 hidden neurons, while larger networks may even degrade prediction accuracy. In addition, compact ANN models are easier to stabilize during training, require lower computational effort, and can be effectively regularized using validation-based early stopping and train/test partitioning.

Because the present model uses only two operating variables, temperature and nanoparticle volume fraction, to predict two thermophysical properties, thermal conductivity and dynamic viscosity, we selected compact single-hidden-layer MLPs rather than wider or deeper networks. This choice is consistent with the nanofluid literature, where low-dimensional property-prediction problems are usually modeled successfully with small MLPs: one hidden layer with four neurons was sufficient for TiO_2/water viscosity, four neurons were also reported as optimal for MgO–water/EG thermal conductivity, and similarly narrow networks have given R or R^2 values close to 0.99 with MSE commonly in the 10^{-6}–10^{-4} range [33, 34]. Even in studies that tested broader architectures, the gains beyond four to five hidden neurons were generally small and sometimes reversed as model

ARTICLE IN PRESS

size increased. By contrast, substantially larger networks have mainly been used for pooled databases with many more inputs and much higher data diversity, such as literature-based models with five to seven inputs and hundreds or thousands of samples. On that basis, MLP 2-3-2 and MLP 2-4-2 were considered appropriate here because they are flexible enough to represent the nonlinear temperature–concentration dependence of Fe_3O_4/water properties, while remaining small enough to limit overfitting, reduce training cost, and preserve interpretability. This justification assumes that the present dataset is of the usual experimental size for single-nanofluid studies and does not include additional descriptors that would require a wider mode.

A logistic sigmoid activation function was used in the hidden layer to capture the nonlinear dependence of the thermophysical properties on temperature and nanoparticle concentration. The logistic function maps the weighted input into a bounded nonlinear range and is appropriate for the normalized input variables employed in this study. For the MLP 2–3–2 model, a hyperbolic tangent function was applied at the output layer because it provides a smooth nonlinear response and is compatible with normalized target values. For the MLP 2–4–2 model, an exponential output function was evaluated to reproduce the positive and nonlinear variation of the predicted thermophysical properties. The final activation-function combinations were retained because they produced the strongest independent testing performance among the compact candidate architectures.

The sensitivity values obtained from the ANN models indicate the relative influence of the input variables on the predicted thermophysical properties of the Fe_3O_4/water ferrofluid. ANN "sensitivity" values in neural-network predictions reflect how strongly each input drives the output, but the exact meaning depends on the method used. For example, Garson's algorithm computes a dimensionless relative importance (normalized sum of absolute weight products), whereas Olden's

ARTICLE IN PRESS

connection-weight method sums signed weight products without normalization. Input-perturbation measures the change in output (or error) when an input is varied slightly. Partial-derivative sensitivities are in units of (Δoutput/Δinput) at a given operating point.

In this study, higher sensitivity values indicate stronger effects of the input parameter on the network output. Therefore, the higher sensitivity of thermal conductivity and dynamic viscosity to temperature than to nanoparticle volume fraction indicates that temperature plays a more dominant role in predicting these properties within the studied operating range. It should be noted that these values mainly represent relative importance indicators inside the ANN structure rather than direct physical rates of change. In addition, the magnitude of the sensitivity values may be affected by the scaling of the input variables and network weights.

Fig. 6 illustrates the value of the sensitivity analysis for two ANNs. As shown in Fig. 6, the maximum and minimum sensitivity values for temperature are 519.498 and 201.352 for MLP2-3-2 and MLP2-4-2, and for volume fraction they are 20.515 and 8.341, respectively. It shows that temperature has a notable influence on thermal conductivity and viscosity, and concludes that MLP2-3-2 is more sensitive than MLP2-4-2.

ARTICLE IN PRESS

ARTICLE IN PRESS

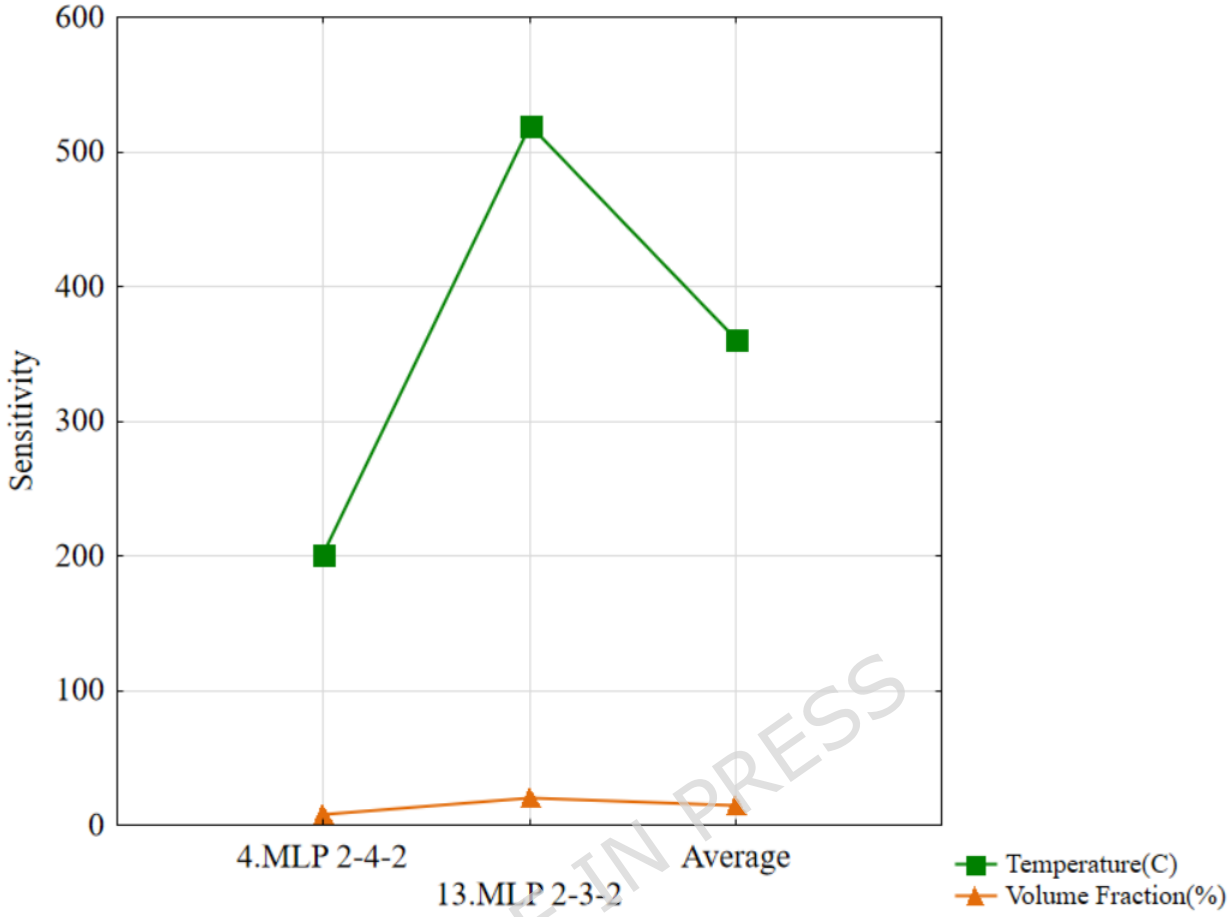


Fig. 6. The sensitivity evolution of MLP 2-3-2 and MLP 2-4-2

The MLP 2-3-2 and MLP 2-4-2 networks provide the best overall performance and the lowest error, with statistical courtship between the train, the validation, the test, and expected and experimental information shown in Fig. 7. The results show that the estimate of the value from the ANN simulation has a strong correlation with the experimental information and the expected data extracted using the ANN and the targets close to 1. Fig. 7a shows the predicted and measured training section. Thermal conductivity and viscosity of an ANN simulation of Fe_3O_4/Water Ferrofluid with three- and four-neuron models. Fig. 7b depicts the results of the validation of dynamic viscosity and thermal conductivity. As shown, the ANN models achieved reasonable overall performance in estimating thermal conductivity, with correlation coefficients of 0.98 and errors of 1.56×10^{-5}. The ANN predicts normalized outputs, then inverse-scales them to physical

ARTICLE IN PRESS

units and compares them to experimental values via the squared-error formula. In summary, an MSE of 1.56×10^{-5} (dimensionless) corresponds to a very small RMSE ($\approx4\times10^{-3}$ in normalized units), reflecting high model accuracy (sub-percent error) comparable to recent nanofluid ANN studies.

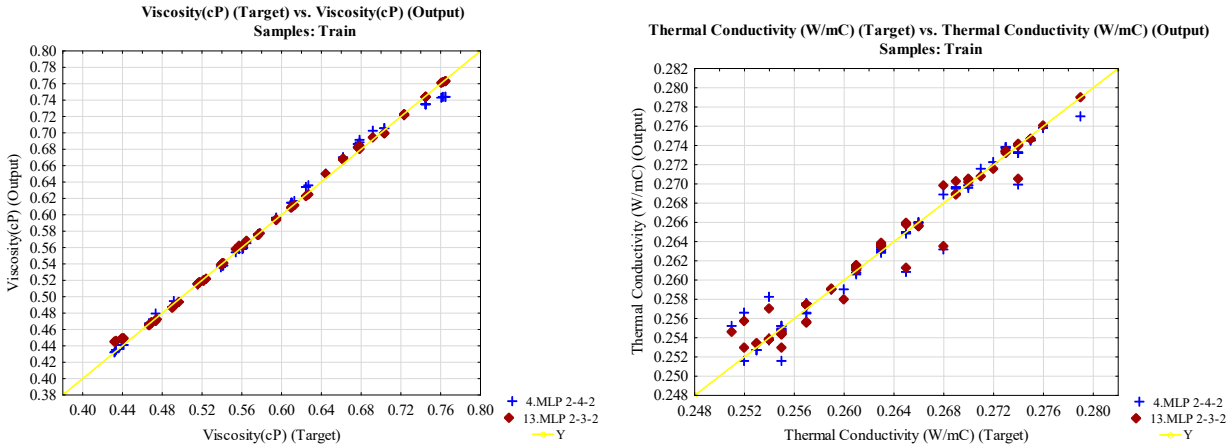
Furthermore, the regression plot results for the test section are shown in Fig. 7c, indicating the correspondence between the ANN outputs and the preferred values. Fig. 7d shows the regression diagram and the correlation problem between the actual output data and the target value for all data based primarily on ANN simulation. This determination indicates agreement between the ANN outputs and the preferred thermal conductivity values for the Fe3O4/Water Ferrofluid. The slope of the regression line is set to 1, yielding an accurate output and shaping the ANN model. Also, almost all the expected information is related to the bisector. The entire section has been further developed compared to the ANNBP model. The correlations for predicting the thermal conductivity and viscosity of Fe_3O_4/Water Ferrofluid based on MLP 2-3-2 and MLP 2-4-2 are shown in Table 3. This table provides a quick estimate of the correlation coefficients and errors for the training, testing, and validation networks. The error values for each training algorithm, along with the training, test, and validation performance results, are presented in this table.

ARTICLE IN PRESS

Table 3. Values estimate the correlation coefficients and errors for simulated ANNs

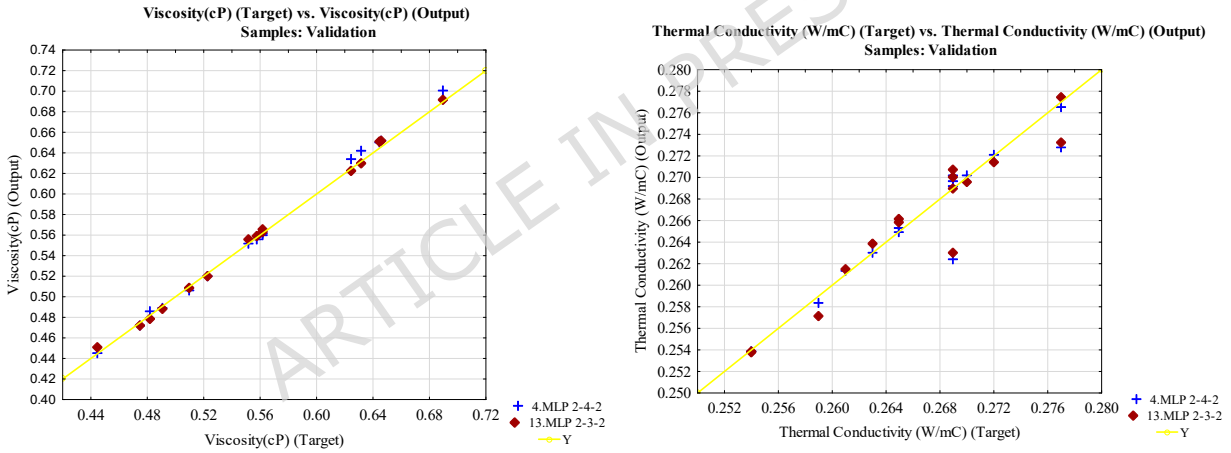
	Training perf.	Test perf.	Validation perf.	Train error	Test error	Validation error	Training algorithm	Hidden activation	Output activation
MLP 2-3-2	0.990	0.977	0.978	2.41×10^{-5}	1.51×10^{-5}	1.56×10^{-5}	BFGS 52	Logistic	Tanh
MLP 2-4-2	0.9811	0.955	0.965	1.32×10^{-6}	1.89×10^{-6}	2.12×10^{-6}	BFGS 78	Logistic	Exponential

ARTICLE IN PRESS



(A) (B)

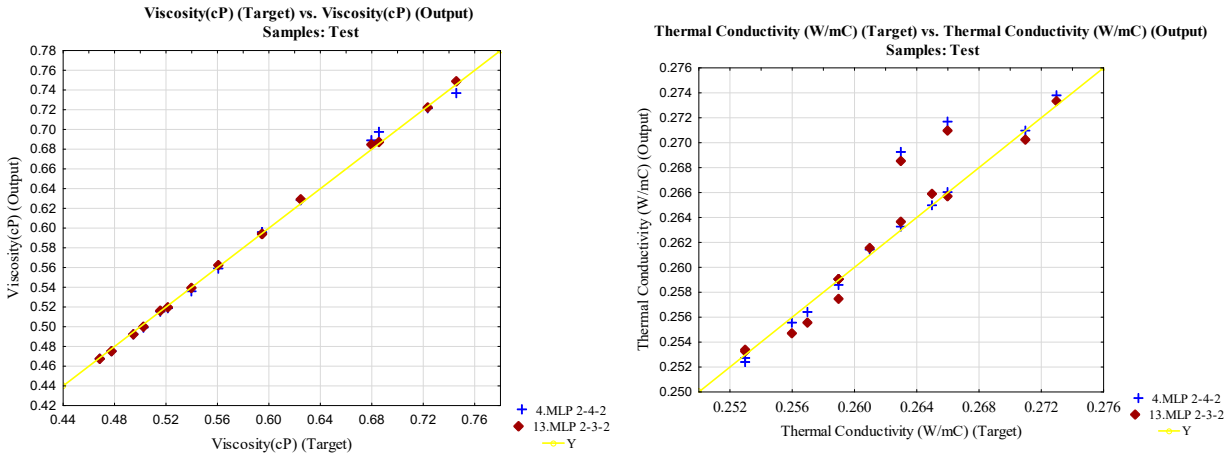
Fig. 7a. The correlation of train data between the actual and the predicted outputs for MLP 2-3-2 and 2-4-2



(A) (B)

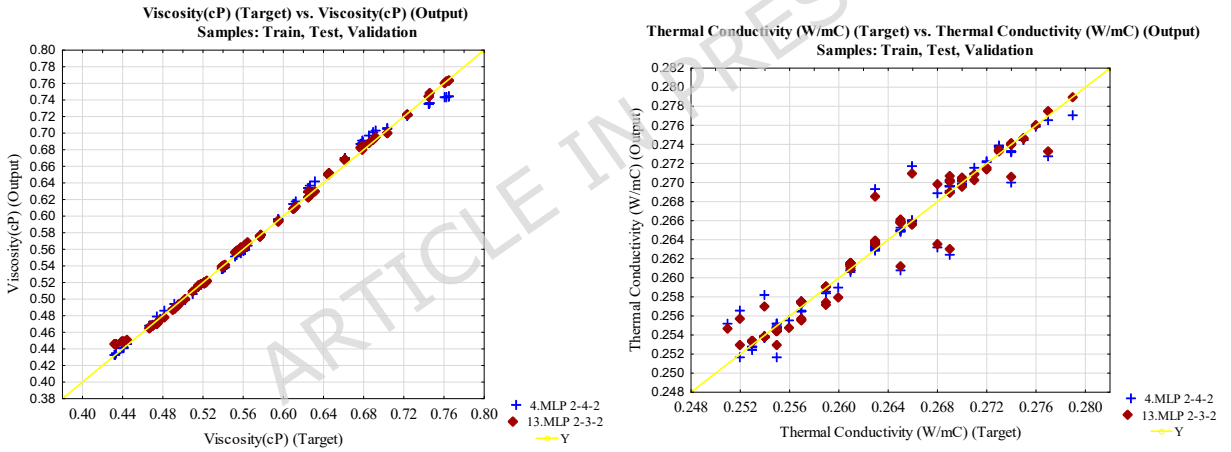
Fig. 7b. The correlation of validation data between the actual and the predicted outputs for MLP 2-3- 2 and 2-4-2

ARTICLE IN PRESS



(A) (B)

Fig. 7c. The correlation of test data between the actual and the predicted outputs for MLP 2-3- 2 and 2-4-2



(A) (B)

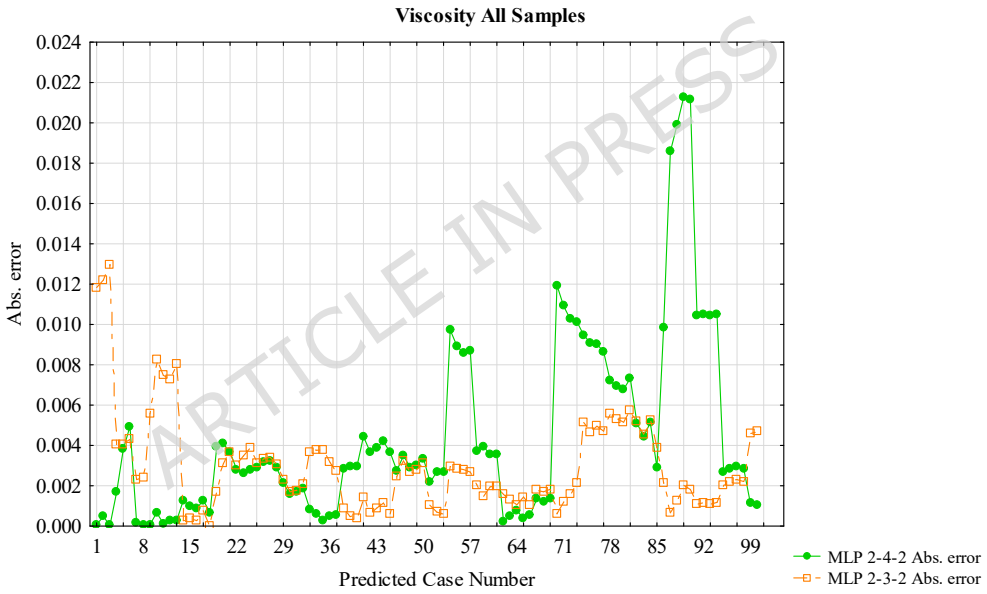
Fig. 7d. The correlation of all data between the actual and the predicted outputs for MLP 2-3- 2 and 2-4-2

Eq. (3) shows that the tanh (hyperbolic tangent activation) has an S-shaped figure, and as a final result, the target trend is captured very precisely as the provided ANN function. Also, the exponential function has an upward trend that grows exponentially. For the targets to show the exponential trend, the ANN uses this function as an activation function. The comparison of the absolute error diagram between the selected networks for all data (a), training data (b), validation

ARTICLE IN PRESS

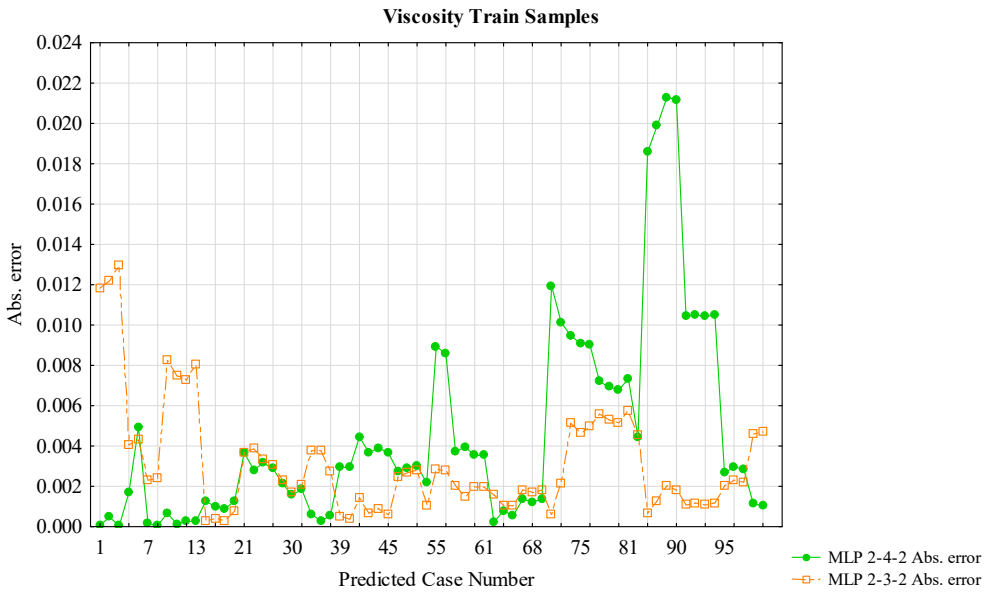
data (c), and test data (d) is shown in Fig. 8. This error value indicates that the ANN is working well and that the method being trained is acceptable. Therefore, the predicted results for thermal conductivity and viscosity from the ANNs provide a good estimate.

Furthermore, the absolute error values of the ANN with 3 and 4 neurons for dynamic viscosity are shown in Fig. 8, where the ANN strategy yields lower absolute errors. From this, it can be concluded that the presented models can accurately predict the nanofluid's dynamic viscosity. The absolute-error simulation of the ANN-estimated Fe3O4/Water Ferrofluid thermal conductivity is illustrated in Fig. 9.

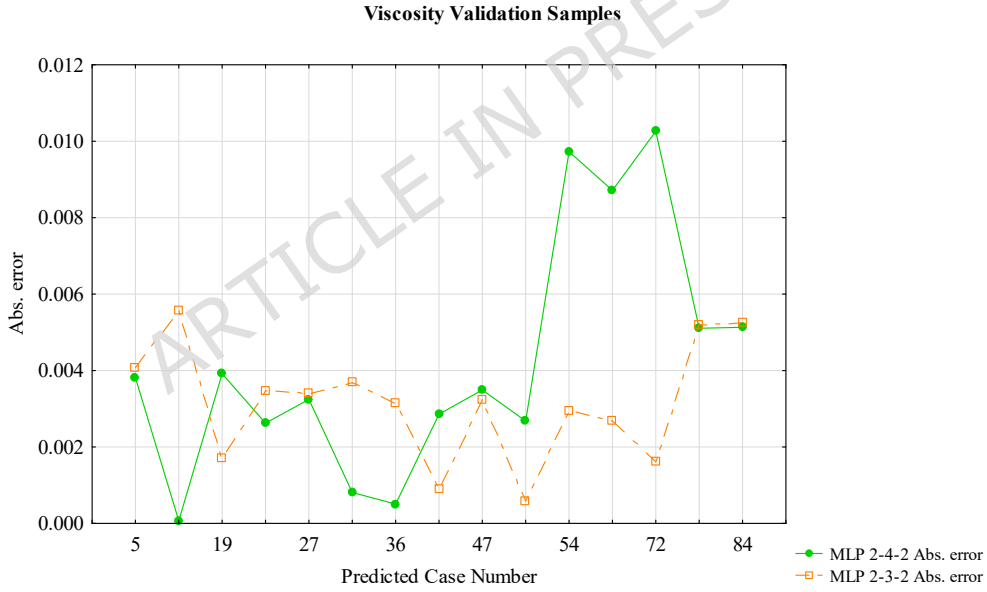


(a)

ARTICLE IN PRESS

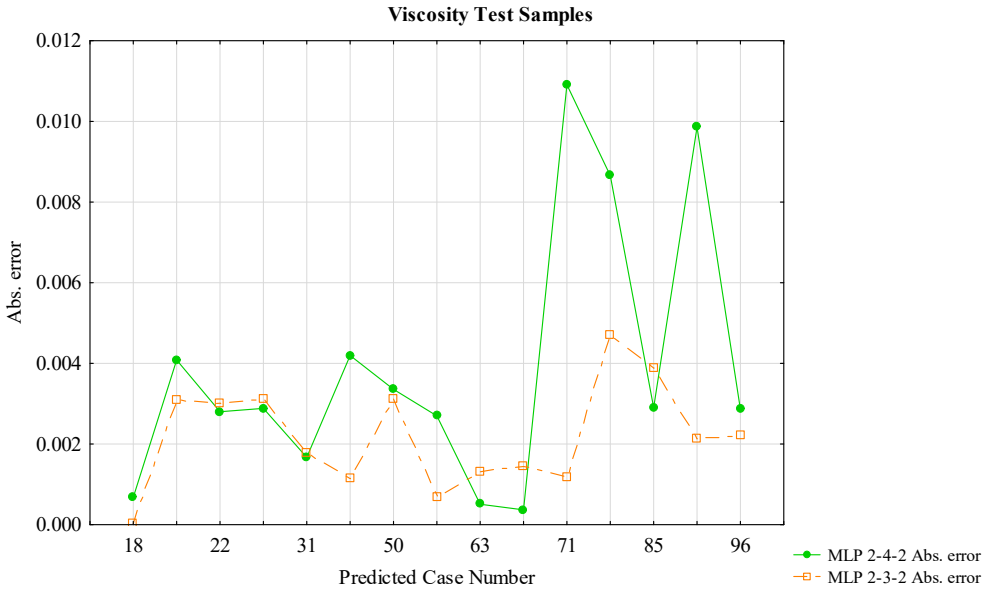


(b)



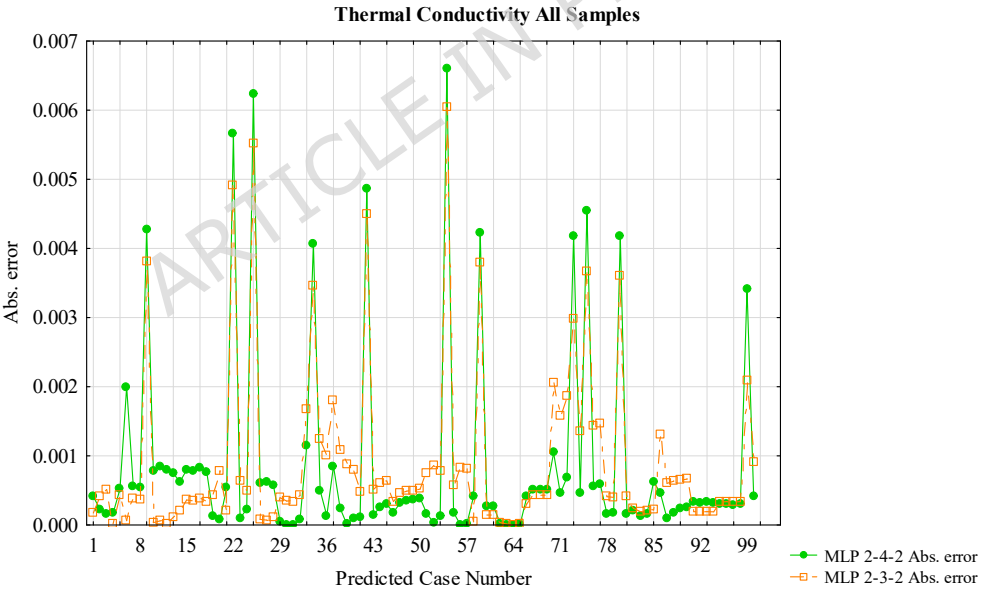
(c)

ARTICLE IN PRESS



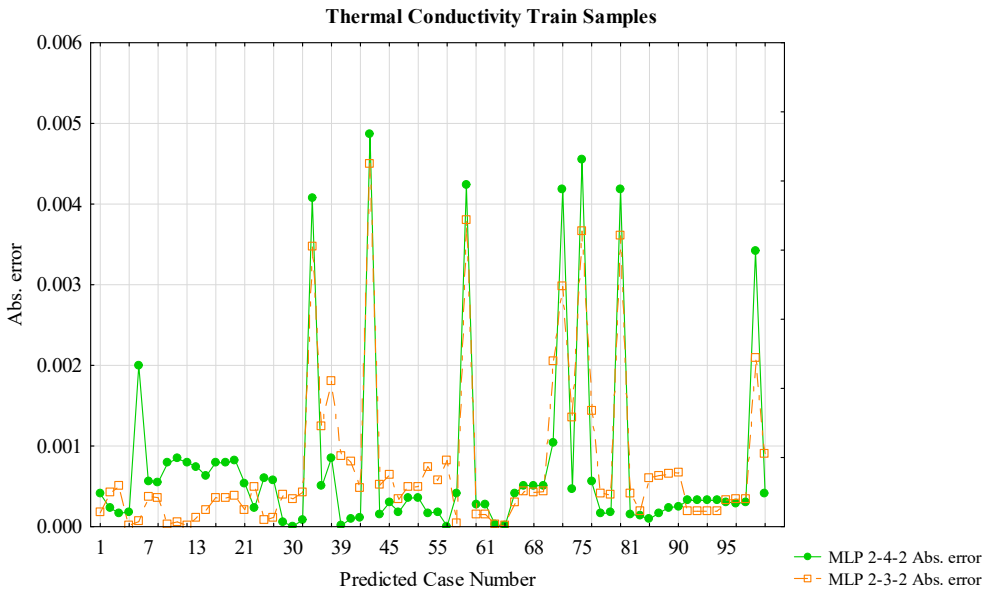
(d)

Fig. 8. MLP 2-3-2 and MLP2-4-2 absolute error value simulation of Fe_3O_4/Water Ferrofluid dynamic viscosity of ANN for all data (a), train data (b), validation data (c), and test data (d)

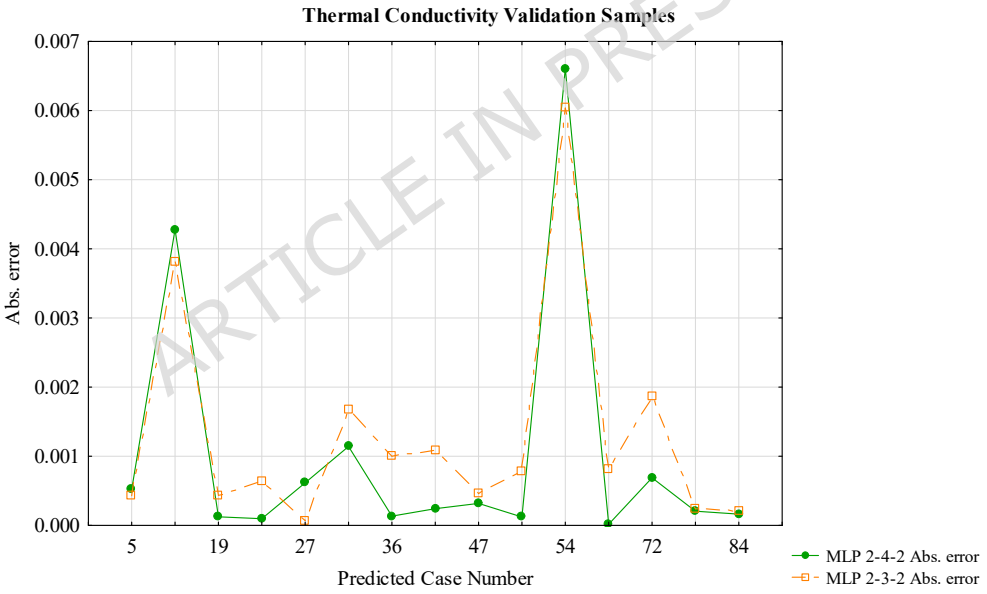


(a)

ARTICLE IN PRESS

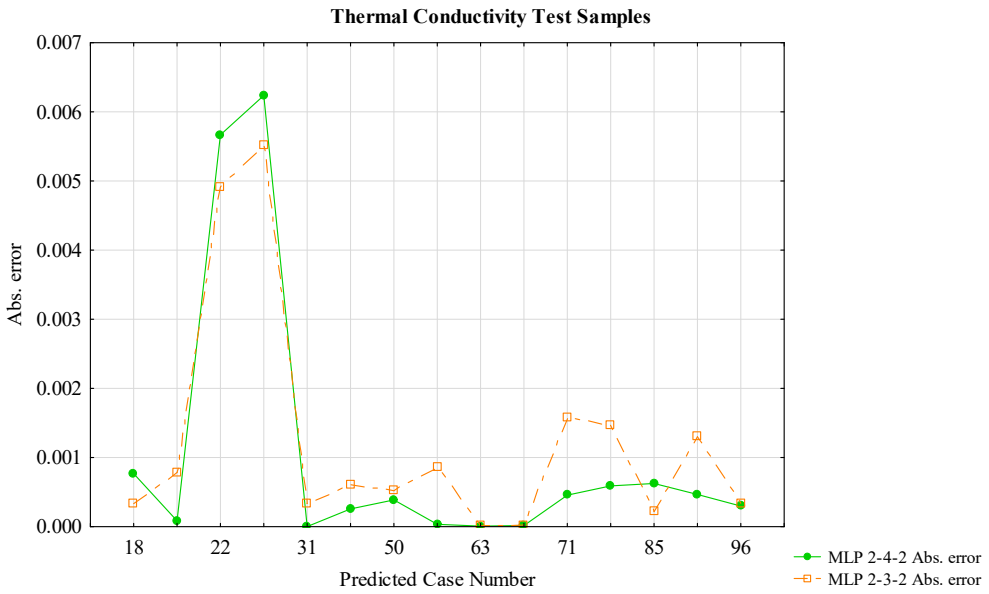


(b)



(c)

ARTICLE IN PRESS



(d)

Fig. 9. MLP 2-3-2 and MLP2-4-2 absolute error value simulation of Fe_3O_4/Water Ferrofluid thermal conductivity of ANN for all data (a), train data (b), validation data (c), and test data (d)

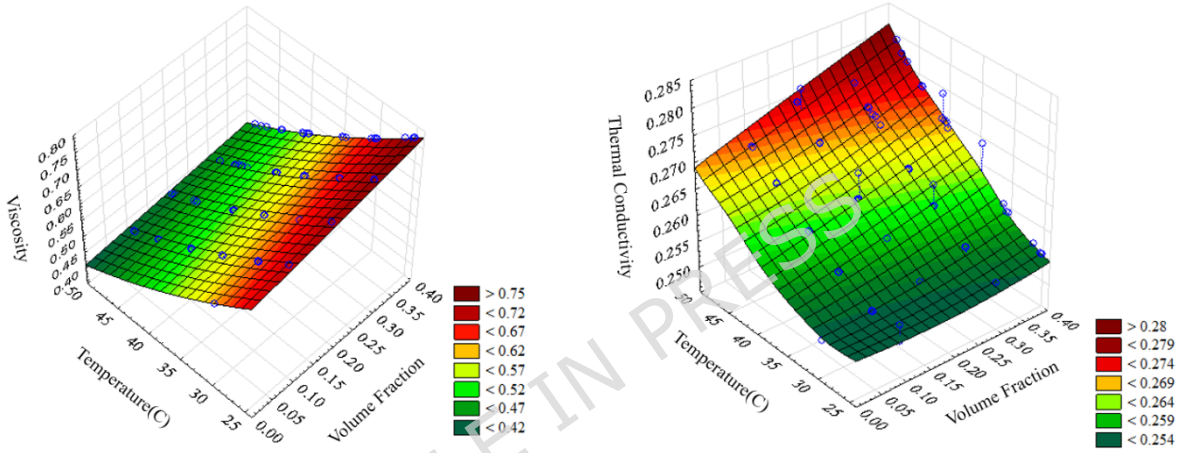
In cutting-edge work, the response surface is modeled using a GLM (General Linear Model). By leveraging capabilities with unique orders, first-class outcomes are associated with a second-order function. Also, to present the fitted surfaces, inputs including φ and temperature, and outputs (thermal conductivity and viscosity) were employed. The fitted surfaces are supplied in Fig. 10 and presented as Eqs. (7) and (8):

$$\text{Thermal Conductivity (W/m°C)} = 0.25225198825 - 0.000384636104399 \times \text{"T (°C)"} + 1.43466014935e\text{-}005 \times \text{"T (°C)"}^2 - 0.0190597269182 \times \text{" } \varphi \text{ (%)"} + 0.0126919405429 \times \text{" } \varphi \text{ (%)"}^2 + 0.000880596155534 \times \text{"T (°C)} \times \varphi \text{ (%)"} \quad (7)$$

$$\text{Viscosity(cP)} = 1.10011091765 - 0.0195683818385 \times \text{"T (°C)"} + 0.000115276812509 \times \text{"T (°C)"}^2 + 0.292426774089 \times \text{" } \varphi \text{ (%)"} + 0.0210319700109 \times \text{" } \varphi \text{ (%)"}^2 - 0.00349683291448 \times \text{"T (°C)} \times \varphi \text{ (%)"} \quad (8)$$

ARTICLE IN PRESS

It can be seen that thermal conductivity increases, especially at higher temperatures, due to the collision between solid and liquid molecules. The contour distribution demonstrates that the relationship between the operating parameters and the output response is nonlinear. The figure also indicates that the effect of temperature becomes more significant at higher nanoparticle concentrations, confirming the coupled influence of these parameters on ferrofluid performance.



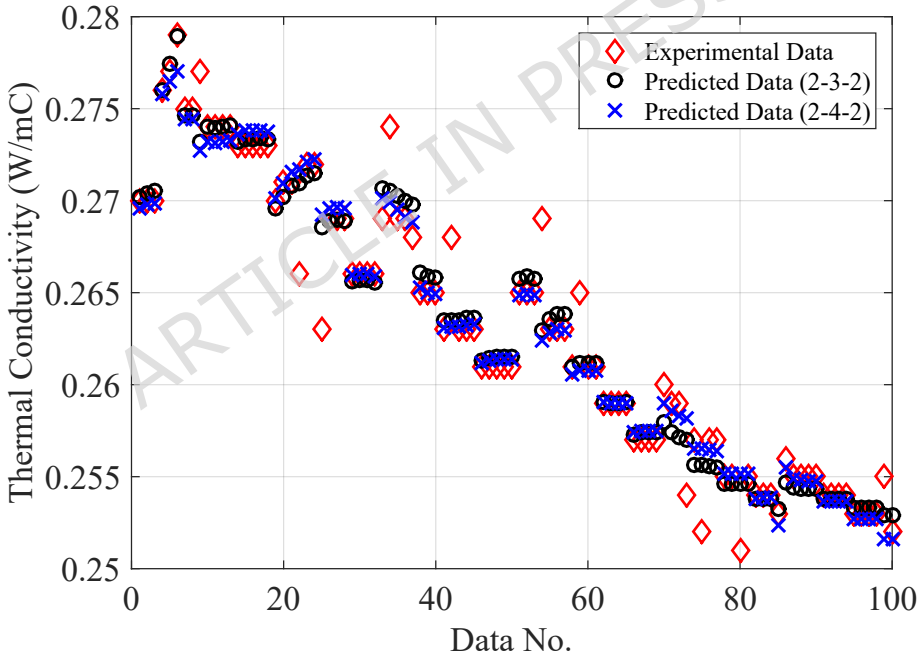
(a) (b)

Fig. 10. 3D plot of the effect of temperature and φ variation on Fe_3O_4/Water Ferrofluid (a) dynamic viscosity (b) thermal conductivity

According to Fig. 11, which compares experimental data with ANN simulation, the simulation results are in good agreement with the laboratory results. Most data points lie close to the regression line, indicating strong agreement between the model outputs and the experimental measurements. The small deviation between predicted and experimental values confirms that the ANN model can reliably estimate the thermophysical properties of Fe_3O_4/water ferrofluid within the studied operating range. Although incorporating dimensionless parameters such as the Reynolds and Prandtl numbers may further improve the generalization capability of ANN-based thermophysical models, the present model already demonstrates satisfactory predictive

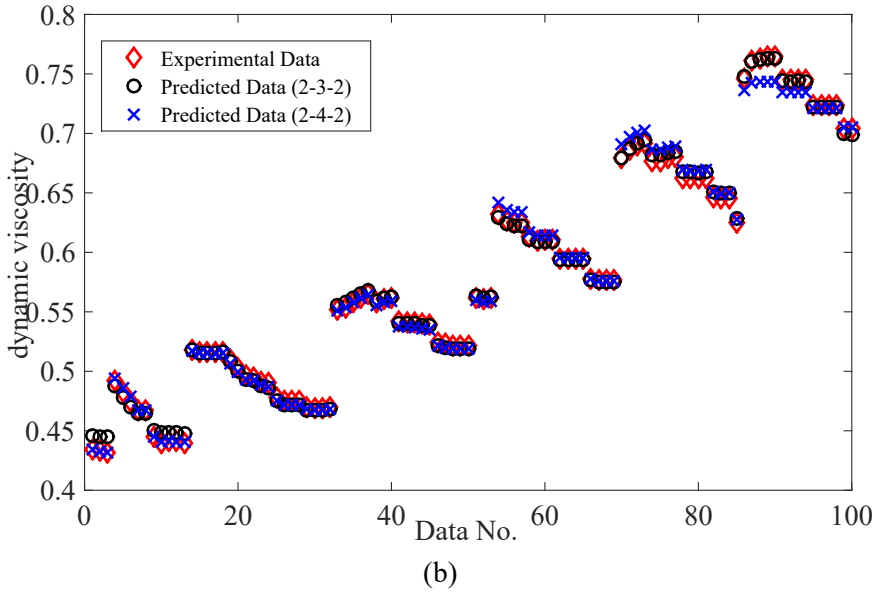
ARTICLE IN PRESS

performance within the studied operating range with only temperature and nanoparticle volume fraction as input variables. Since the current investigation focuses primarily on predicting thermal conductivity and dynamic viscosity under controlled experimental conditions, the selected input parameters were sufficient to capture the dominant nonlinear behavior of the Fe_3O_4/water ferrofluid. The obtained correlation coefficients and low MSE values confirm that the developed ANN architectures provide reliable and accurate predictions without the need for additional dimensionless descriptors. Nevertheless, integrating dimensionless analysis may be considered in future studies aimed at extending the model's applicability to broader flow and heat-transfer conditions.



(a)

ARTICLE IN PRESS



(b)

Fig. 11. Differences between laboratory data and ANN simulations for (a) thermal conductivity and (b) dynamic Fe_3O_4/Water ferrofluid viscosity.

4. Dsiccusion

4.1. Thermal Conductivity: Experimental Results and Physical Interpretation

The experimental results demonstrated that the thermal conductivity of the Fe_3O_4/water ferrofluid increased with both nanoparticle volume fraction and temperature. At a constant temperature, increasing the Fe_3O_4 concentration enhanced the effective thermal conductivity because the dispersed solid particles possessed a higher intrinsic thermal conductivity than the base fluid. The addition of nanoparticles therefore introduced supplementary conductive pathways through the suspension and reduced the overall thermal resistance of the fluid. The enhancement became more noticeable at higher nanoparticle concentrations, where the average distance between adjacent particles was reduced, and particle-mediated energy transport became more significant.

Temperature also exerted a positive effect on the thermal conductivity of the Ferrofluid. Increasing the temperature intensified molecular activity in the base fluid and increased the mobility of the suspended nanoparticles. These effects can improve energy exchange at the particle–fluid interface

ARTICLE IN PRESS

and facilitate heat transport through the suspension. However, the contribution of Brownian motion should be interpreted together with other mechanisms, including static conduction through the nanoparticles, particle–fluid interfacial layers, and the possible formation of temporary conductive particle networks. The smooth variation of thermal conductivity over the investigated operating range indicates that the experimental data followed a consistent thermophysical trend without abrupt changes.

The simultaneous influence of temperature and nanoparticle concentration was nonlinear. At relatively low particle concentrations, temperature remained an important factor in improving thermal conductivity, whereas at higher concentrations, the contribution of the dispersed Fe_3O_4 phase became increasingly significant. The interaction between these two variables indicates that their effects should not be assessed independently when designing ferrofluid-based thermal systems. Although a higher particle concentration improves thermal conductivity, its benefit must be evaluated alongside the accompanying increase in viscosity and the resulting pumping-power requirement. Therefore, the most suitable operating condition is not necessarily associated with the maximum thermal conductivity but with an appropriate balance between thermal enhancement and flow resistance.

ARTICLE IN PRESS

4.2. Dynamic Viscosity: Experimental Results and Physical Interpretation

The dynamic viscosity of the Fe_3O_4/water ferrofluid exhibited an opposite temperature dependence to thermal conductivity. At a constant nanoparticle volume fraction, viscosity decreased as the temperature increased. This behavior is primarily attributed to the reduction in the viscosity of the water-based continuous phase at elevated temperatures. Increasing temperature provides greater kinetic energy to the fluid molecules, weakens the effective intermolecular resistance, and

ARTICLE IN PRESS

increases molecular mobility. Consequently, the suspension flows more readily and exhibits lower dynamic viscosity.

In contrast, increasing the nanoparticle volume fraction resulted in higher dynamic viscosity at a given temperature. A greater concentration of Fe_3O_4 nanoparticles increases the effective solid content of the suspension and strengthens hydrodynamic resistance, particle–fluid interactions, and particle–particle interactions. The reduced distance between particles at higher concentrations also increases the probability of temporary particle structures or agglomerates, which can restrict fluid movement and increase resistance to deformation. Therefore, the concentration-related increase in viscosity is physically consistent with the behavior expected for a particle-containing suspension.

The effects of temperature and volume fraction should be considered simultaneously when evaluating the practical performance of the Ferrofluid. Increasing the nanoparticle concentration improves thermal conductivity but also increases viscosity, which may result in a higher pressure drop and greater pumping-power consumption. Conversely, increasing temperature reduces viscosity while also improving thermal conductivity, making elevated temperature favorable from both thermal and flow perspectives within the investigated range. Nevertheless, the developed experimental relationships are valid only for the preparation procedure and operating conditions considered in this study. Changes in particle size, surfactant concentration, sonication conditions, aggregation state, or suspension stability could alter the measured viscosity behavior.

ARTICLE IN PRESS

4.3. ANN Prediction Results and Performance Discussion

Twenty feed-forward multilayer perceptron configurations were evaluated to model the nonlinear relationship between temperature and nanoparticle volume fraction as inputs and thermal

ARTICLE IN PRESS

conductivity and dynamic viscosity as outputs. The final models were selected by considering testing and validation performance, prediction error, and architectural complexity simultaneously. Network 13, with an MLP 2–3–2 architecture, achieved training, validation, and testing performance coefficients of 0.992973, 0.978419, and 0.977399, respectively, with corresponding MSE values of 9.37×10^{-6}, 8.14×10^{-6}, and 5.28×10^{-6}. Network 4, with an MLP 2–4–2 architecture, achieved performance coefficients of 0.990473, 0.978377, and 0.976804 for the training, validation, and testing subsets, respectively. Although some larger networks produced lower MSE values, they did not improve independent testing performance; therefore, the compact MLP 2–3–2 and MLP 2–4–2 networks provided a more appropriate balance between accuracy and model complexity.

The ANN predictions agreed closely with the experimental measurements, as demonstrated by the predicted values lying close to the line of perfect agreement in the regression plots and the relatively small deviations observed in the absolute-error plots. The comparable training, validation, and testing performance indicates that the selected models achieved satisfactory generalization without merely memorizing the training observations. Moreover, the ANN models reproduced the physically expected trends of increasing thermal conductivity with temperature and nanoparticle concentration and decreasing viscosity with increasing temperature. Nevertheless, the models should be used only within the experimental ranges represented in the dataset because their reliability has not been established for extrapolation. Additional inputs such as particle size, sonication duration, surfactant concentration, shear rate, and suspension stability could be considered in future studies to improve their broader applicability.

5- Conclusion

ARTICLE IN PRESS

With advances in research, nanofluids can now be made by suspending metal oxide nanoparticles and even carbon nanorods. Among these, nanofluids containing Fe_3O_4 nanoparticles are of particular interest to researchers due to their unique properties, including favorable magnetic properties and environmental friendliness. This study aimed to develop an ANN model to determine the dynamic viscosity and thermal conductivity of Fe_3O_4/Water ferrofluid. In an actual dataset obtained from an experiment, this relationship was complex and required an artificial intelligence method to build a reliable model for analyzing the problem. In this study, the dynamic viscosity and thermal conductivity of Fe_3O_4/Water ferrofluid were measured at T= 24 °C to 50 °C for suspensions with φ=0.05% to 4%. The following conclusions can be summarized based on the obtained results:

- At excessive temperatures, the maximum value of thermal conductivity is reached while the φ increases to the maximum value.
- Unlike thermal conductivity, viscosity has its lowest value at high temperatures.
- The φ changes from φ =0.05% to 4.0%, and the dynamic viscosity increases from 0.43 to 0.77 cP.
- At low temperatures, excessive thermal conductivity can be achieved if the φ is the highest.
- By exceeding the temperature of 30 °C, high thermal conductivity can be achieved even in small proportions of the φ.
- The sensitivity analysis's maximum and minimum values for temperature are 519.498858 and 201.352559 for MLP2-3-2 and MLP2-4-2, respectively, and the volume fraction is 20.5154254 and 8.34135455, respectively.

ARTICLE IN PRESS

ARTICLE IN PRESS

- The ANN models showed reasonable overall performance in estimating thermal conductivity, with correlation coefficients of 0.98 and errors of $1.56\times10^{\wedge-5}$.
- The network is well trained, employing the Tanh activation function for the hidden layer and the exponential function for the output.
- The results indicate that the ANN model can accurately predict dynamic viscosity and thermal conductivity based on the Fe_3O_4/Water ferrofluid parameters considered in this study.
- A comparative study of laboratory data and ANN simulations of thermal conductivity and dynamic viscosity of Fe_3O_4/Water ferrofluid was presented.
- The results of the current study were in good agreement with data obtained through direct experimental simulations.

ARTICLE IN PRESS

Declaration

Ethics approval and consent to participate: N/A

• **Consent for publication:** N/A

• **Competing interests:** N/A

• **Funding:** N/A

• **Authors' contributions:**

All authors reviewed the manuscript.: Funding acquisition, Formal analysis, Data curation, Conceptualization. Writing – original draft; Writing – review and editing

• **Acknowledgments:** N/A

• **Availability of data and material:** N/A

Data Availability Statement

ARTICLE IN PRESS

The data that support the findings of this study are available from the corresponding author, upon reasonable request.

Funding Declaration: Not Applicable

References

[1] C. Lin, J. Zhou, Q. Lu, M.K. Khabaz, A.K. Andani, M. Al-Yasiri, G. Pan, Thermal conductivity prediction of WO3-CuO-Ag (35: 40: 25)/Water hybrid ternary nanofluid with Artificial Neural Network and backpropagation algorithm, Materials Today Communications, DOI (2023) 106807.
[2] H. Qing, S. Hamedi, S.A. Eftekhari, S. Alizadeh, D. Toghraie, M. Hekmatifar, A.N. Ahmed, A. Khan, A well-trained feed-forward perceptron Artificial Neural Network (ANN) for prediction the dynamic viscosity of Al2O3–MWCNT (40: 60)-Oil SAE50 hybrid nano-lubricant at different volume fraction of nanoparticles, temperatures, and shear rates, International Communications in Heat and Mass Transfer, 128 (2021) 105624.
[3] A.R. Rahmati, O.A. Akbari, A. Marzban, D. Toghraie, R. Karimi, F. Pourfattah, Simultaneous investigations the effects of non-Newtonian nanofluid flow in different volume fractions of solid nanoparticles with slip and no-slip boundary conditions, Thermal Science and Engineering Progress, 5 (2018) 263-277.
[4] A. Pare, S.K. Ghosh, A unique thermal conductivity model (ANN) for nanofluid based on experimental study, Powder Technology, 377 (2021) 429-438.
[5] C. Yang, W. Li, A. Nakayama, Convective heat transfer of nanofluids in a concentric annulus, International journal of thermal sciences, 71 (2013) 249-257.
[6] N.A.C. Sidik, I.M. Adamu, M.M. Jamil, G. Kefayati, R. Mamat, G. Najafi, Recent progress on hybrid nanofluids in heat transfer applications: a comprehensive review, International Communications in Heat and Mass Transfer, 78 (2016) 68-79.
[7] B. Bakthavatchalam, K. Habib, R. Saidur, B.B. Saha, K. Irshad, Comprehensive study on nanofluid and ionanofluid for heat transfer enhancement: A review on current and future perspective, Journal of Molecular Liquids, 305 (2020) 112787.
[8] A.A. Alrashed, O.A. Akbari, A. Heydari, D. Toghraie, M. Zarringhalam, G.A.S. Shabani, A.R. Seifi, M. Goodarzi, The numerical modeling of water/FMWCNT nanofluid flow and heat transfer in a backward-facing contracting channel, Physica B: Condensed Matter, 537 (2018) 176-183.
[9] M. Sheikholeslami, R. Ellahi, K. Vafai, Study of Fe3O4-water nanofluid with convective heat transfer in the presence of magnetic source, Alexandria Engineering Journal, 57 (2018) 565-575.
[10] L.S. Sundar, M.K. Singh, A.C. Sousa, Investigation of thermal conductivity and viscosity of Fe3O4 nanofluid for heat transfer applications, International communications in heat and mass transfer, 44 (2013) 7-14.
[11] A. Shahsavar, M. Bahiraei, Experimental investigation and modeling of thermal conductivity and viscosity for non-Newtonian hybrid nanofluid containing coated CNT/Fe3O4 nanoparticles, Powder Technology, 318 (2017) 441-450.
[12] S. Tian, N.I. Arshad, D. Toghraie, S.A. Eftekhari, M. Hekmatifar, Using perceptron feed-forward Artificial Neural Network (ANN) for predicting the thermal conductivity of graphene oxide-Al2O3/water-ethylene glycol hybrid nanofluid, Case Studies in Thermal Engineering, 26 (2021) 101055.
[13] M.H. Esfe, A. Alirezaie, D. Toghraie, Thermal conductivity of ethylene glycol based nanofluids containing hybrid nanoparticles of SWCNT and Fe3O4 and its price-performance

ARTICLE IN PRESS

analysis for energy management, Journal of Materials Research and Technology, 14 (2021) 1754-1760.
[14] D.S. Toghraie, N. Sina, M. Mozafarifard, A.a. Alizadeh, F. Soltani, M.A. Fazilati, Prediction of dynamic viscosity of a new non-Newtonian hybrid nanofluid using experimental and artificial neural network (ANN) methods, Heat Transfer Research, 51 (2020).
[15] S.H. Rostamian, M. Biglari, S. Saedodin, M.H. Esfe, An inspection of thermal conductivity of CuO-SWCNTs hybrid nanofluid versus temperature and concentration using experimental data, ANN modeling and new correlation, Journal of Molecular Liquids, 231 (2017) 364-369.
[16] G. Fan, A. El-Shafay, S.A. Eftekhari, M. Hekmatifar, D. Toghraie, A.S. Mohammed, A. Khan, A well-trained artificial neural network (ANN) using the trainlm algorithm for predicting the rheological behavior of water–Ethylene glycol/WO3–MWCNTs nanofluid, International Communications in Heat and Mass Transfer, 131 (2022) 105857.
[17] M. Hemmat Esfe, M. Hajian, D. Toghraie, M. Khaje khabaz, A. Rahmanian, M. Pirmoradian, H. Rostamian, Prediction the dynamic viscosity of MWCNT-Al2O3 (30:70)/ Oil 5W50 hybrid nano-lubricant using Principal Component Analysis (PCA) with Artificial Neural Network (ANN), Egyptian Informatics Journal, DOI https://doi.org/10.1016/j.eij.2022.03.004(2022).
[18] M.H. Esfe, M.K. khabaz, R. Esmaily, S.T. Mahabadi, D. Toghraie, A. Rahmanian, M.A. Fazilati, Application of Artificial Intelligence and Using Optimal ANN to Predict the Dynamic Viscosity of MWCNT-ZnO (50-50)/oil SAE50 Hybrid Nano-lubricant, Colloids and Surfaces A: Physicochemical and Engineering Aspects, DOI https://doi.org/10.1016/j.colsurfa.2022.129115(2022) 129115.
[19] S.A.M. Hejazi, A. Feyzpour, M. Khaje khabaz, A. Eslami, M. Fouladgar, S.A. Eftekhari, D. Toghraie, Numerical Investigation of Rigidity and Flexibility Parameters Effect on Superstructure Foundation Behavior Using Three-Dimensional Finite Element Method, Case Studies in Construction Materials, DOI https://doi.org/10.1016/j.cscm.2023.e01867(2023) e01867.
[20] S. Rostami, D. Toghraie, B. Shabani, N. Sina, P. Barnoon, Measurement of the thermal conductivity of MWCNT-CuO/water hybrid nanofluid using artificial neural networks (ANNs), Journal of Thermal Analysis and Calorimetry, 143 (2021) 1097-1105.
[21] N. Kumar, S.S. Sonawane, S.H. Sonawane, Experimental study of thermal conductivity, heat transfer and friction factor of Al2O3 based nanofluid, International Communications in Heat and Mass Transfer, 90 (2018) 1-10.
[22] F. Derakhshanfard, A. Mehralizadeh, Application of artificial neural networks for viscosity of crude oil-based nanofluids containing oxides nanoparticles, Journal of Petroleum Science and Engineering, 168 (2018) 263-272.
[23] M. Goodarzi, D. Toghraie, M. Reiszadeh, M. Afrand, Experimental evaluation of dynamic viscosity of ZnO–MWCNTs/engine oil hybrid nanolubricant based on changes in temperature and concentration, Journal of Thermal Analysis and Calorimetry, 136 (2019) 513-525.
[24] M.H. Esfe, S.A. Eftekhari, M. Hekmatifar, D. Toghraie, A well-trained artificial neural network for predicting the rheological behavior of MWCNT–Al2O3 (30–70%)/oil SAE40 hybrid nanofluid, Scientific Reports, 11 (2021) 1-11.
[25] J. Philip, Magnetic nanofluids (Ferrofluids): Recent advances, applications, challenges, and future directions, Advances in Colloid and Interface Science, 311 (2023) 102810.
[26] L. Chang, W. Yang, M.K. Khabaz, S.A. Eftekhari, T. Alkhalifah, Y. Khairy, Introducing an integrated self-organizing map and radial basis function network for accurate prediction of water-Fe3O4 nanofluid viscosity versus solid volume fraction and temperature, Renewable and Sustainable Energy Reviews, 209 (2025) 115119.

ARTICLE IN PRESS

[27] Z. Wang, H.O. Shami, K.J. Kazim, A. Basem, H.J. Al-fanhrawi, K.E.C. Dacto, S. Salahshour, M. Khajehkhabaz, S.A. Eftekhari, Using different Heuristic strategies and an adaptive Neuro-Fuzzy inference system for multi-objective optimization of Hybrid Nanofluid to provide an efficient thermal behavior, Swarm and Evolutionary Computation, 86 (2024) 101536.
[28] A. Alkhafaji, M.K. Khabaz, M. Alsaadi, N.S.S. Singh, M.M. Adafah, S.A. Eftekhari, M. Taner, S. Salahshour, Exploring the impact of different clustering techniques and their parameters on the precision of viscosity predictions for water-based nanofluids containing magnetic nanoparticles, Systems and Soft Computing, DOI (2026) 200523.
[29] L. Abidoye, F. Mahdi, M. Idris, O. Alabi, A. Wahab, ANN-derived equation and ITS application in the prediction of dielectric properties of pure and impure CO2, Journal of Cleaner Production, 175 (2018) 123-132.
[30] M. Khajekhabaz, A. Eftekhari, M. Hashemian, Free Vibration Analysis of Sandwich Micro Beam with Piezoelectric Based on Modified Couple Stress Theory and Surface Effects, Journal of Simulation and Analysis of Novel Technologies in Mechanical Engineering, 10 (2018) 33-48.
[31] J.J. Hopfield, Artificial neural networks, IEEE Circuits and Devices Magazine, 4 (1988) 3-10.
[32] S. Li, A. Basem, A.K.J. Al-Nussairi, N.S.S. Singh, A.R. Hasson, M. Norberdiyeva, M. Khajehkhabaz, S. Salahshour, H. Sahramaneshi, Prediction methods and influencing factors on the viscosity of nanofluids using machine learning: A comprehensive review, International Communications in Heat and Mass Transfer, 176 (2026) 111201.
[33] Y. Zhang, K.A. Hammoodi, S.M. Sajadi, Z. Li, D.J. Jasim, N. Nasajpour-Esfahani, S. Salahshour, S.A. Eftekhari, M.K. Khabaz, Obtaining an accurate prediction model for viscosity of a new nano-lubricant containing multi-walled carbon nanotube-titanium dioxide nanoparticles with oil SAE50, Tribology International, 191 (2024) 109185.
[34] J. Gao, D.J. Jasim, S.M. Sajadi, S.A. Eftekhari, M. Hekmatifar, S. Salahshour, F.T. Shahdost, D. Toghraie, An RBF-based artificial neural network for prediction of dynamic viscosity of MgO/SAE 5W30 oil hybrid nano-lubricant to obtain the best performance of energy systems, Materials Today Communications, 38 (2024) 107836.

ARTICLE IN PRESS